J. Fluid Mech. (1997), *vol.* 337, *pp.* 303–332

Energy transfer in rotating turbulence

By CLAUDE CAMBON[1], N. N. MANSOUR[2] AND F. S. GODEFERD[1]

[1]Laboratoire de Mécanique des Fluides et d'Acoustique, UMR5509, École Centrale de Lyon, 69131 Ecully cedex, France

[2]NASA-Ames Research Center, Moffett Field, CA 94035, USA

(Received 5 September 1995 and in revised form 10 October 1996)

The influence of rotation on the spectral energy transfer of homogeneous turbulence is investigated in this paper. Given the fact that linear dynamics, e.g. the inertial waves regime found in an RDT (rapid distortion theory) analysis, cannot affect a homogeneous isotropic turbulent flow, the study of nonlinear dynamics is of prime importance in the case of rotating flows. Previous theoretical (including both weakly nonlinear and EDQNM theories), experimental and DNS (direct numerical simulation) results are collected here and compared in order to give a self-consistent picture of the nonlinear effects of rotation on turbulence.

The inhibition of the energy cascade, which is linked to a reduction of the dissipation rate, is shown to be related to a damping of the energy transfer due to rotation. A model for this effect is quantified by a model equation for the derivative-skewness factor, which only involves a *micro*-Rossby number $Ro^\omega = \omega'/(2\Omega)$ – ratio of r.m.s. vorticity and background vorticity – as the relevant rotation parameter, in accordance with DNS and EDQNM results.

In addition, anisotropy is shown also to develop through nonlinear interactions modified by rotation, in an intermediate range of Rossby numbers ($Ro^L < 1$ and $Ro^\omega > 1$), which is characterized by a *macro*-Rossby number Ro^L based on an integral lengthscale L and the micro-Rossby number previously defined. This anisotropy is mainly an angular drain of spectral energy which tends to concentrate energy in the wave-plane normal to the rotation axis, which is exactly both the slow and the two-dimensional manifold. In addition, a polarization of the energy distribution in this slow two-dimensional manifold enhances horizontal (normal to the rotation axis) velocity components, and underlies the anisotropic structure of the integral length-scales. Finally a generalized EDQNM (eddy damped quasi-normal Markovian) model is used to predict the underlying spectral transfer structure and all the subsequent developments of classic anisotropy indicators in physical space. The results from the model are compared to recent LES results and are shown to agree well. While the EDQNM2 model was developed to simulate 'strong' turbulence, it is shown that it has a strong formal analogy with recent weakly nonlinear approaches to wave turbulence.

1. Introduction

The dominance of mean rotation over mean strain can be found in many flows of practical interest. It can be shown that conventional one-point closure models cannot predict the effects of rotation on the turbulence statistics. In addition, many recent studies have shown that mean rotation is an important factor in certain mechanisms

of flow instability. The study of rotating flows is therefore interesting from the point of view of both topological flow structure and turbulence modelling in fields as diverse as engineering (e.g. turbomachinery, reciprocating engines with swirl and tumble), geophysics and astrophysics.

The simplest flow where the effects of rotation on turbulence can be isolated is the case of initially unstructured turbulence (isotropic) subjected to rotation. While the Coriolis force has been introduced in theoretical and numerical approaches from the initial time, we consider initially isotropic turbulence in an already spun-up fluid, such as grid turbulence in a rotating tank – see the experiment by Hopfinger, Browand & Gagne (1982). This flow has been extensively investigated theoretically, including both linear (Greenspan 1968), and weakly nonlinear theories of resonant waves (Waleffe 1991, 1993, hereafter referred to as Waleffe). Linear RDT (rapid distortion theory) and nonlinear EDQNM (eddy damped quasi-normal Markovian) models were developed to study these flows. These models can be shown to have a close connection with the theoretical (weak turbulence) analyses but were developed to simulate developed turbulence (Itsweire, Chabert & Gence 1979; Cambon & Jacquin 1989; Mansour, Cambon & Speziale 1991*a*, *b*; Mansour, Shih & Reynolds 1991*c*). The same class of flows was also investigated experimentally by Wigeland & Nagib (1978), Jacquin *et al.* (1990) and Veeravalli (1991), and simulated using DNS (direct numerical simulations) and LES (large-eddy simulations) methodologies by various groups (Bardina, Ferziger & Rogallo 1985; Dang & Roy 1985; Speziale, Mansour & Rogallo 1987; Mansour *et al.* 1991*a*, *b*; Bartello, Métais & Lesieur 1994). Of course, the previous list of references is not comprehensive, but a brief survey of existing literature is easier if it is restricted to homogeneous flows (the experiment by Hopfinger *et al.* 1982 cannot be therefore included). In what follows, emphasis is placed on fundamental effects of background rotation, on flows without mean gradients (shear, deformation, temperature gradient), walls, stirring forces or pre-existing organized eddies.

The studies of Jacquin, Leuchter & Geoffroy (1989), Jacquin *et al.* (1990) and Mansour *et al.* (1991*b*), have suggested a new insight into the problem of transition from three-dimensional to two-dimensional structure caused by pure Coriolis effects, a problem which is often avoided by invoking the classic Proudman–Taylor theorem. The main finding is that the departure from isotropy (under rotation), which is linked to the first phase of the transition process, is mediated by nonlinear interactions and, therefore, only occurs at intermediate Rossby numbers for sufficiently high Reynolds numbers. If the rotation is too weak, so that a *macro*-Rossby number $Ro^L = u'/(2\Omega L)$ is larger than 1, the rotation cannot affect the dynamics of three-dimensional isotropic freely decaying turbulence. If the rotation is too strong, so that a *micro*-Rossby number $Ro^\lambda = u'/(2\Omega\lambda) \propto Ro^\omega = \omega'/2\Omega$ is smaller than 1, the nonlinear terms are completely damped through scrambling effects of inertial waves, so that a pure viscous decay is obtained and no transition can develop. Here u' and ω' are r.m.s. velocity and vorticity fluctuations, whereas L and λ denote a typical integral lengthscale and a typical Taylor microscale, respectively. At the intermediate range ($Ro^L < 1$ and $Ro^\lambda > 1$), the width of which depends on the Reynolds number through the ratio L/λ (so that $Ro^\omega \sim Ro^L Re^{1/2}$), anisotropy develops in agreement with the beginning of the transition to two-dimensional. This anisotropy is first detected by the departure of the integral lengthscales in several directions from their isotropic values.

The role of the Reynolds number is clear in recent 128^3 and 256^3 DNS by Mansour *et al.* (1991), but these DNS runs are limited to only moderate Reynolds numbers, since they started at the end of an isotropic precomputation without rotation. In order to reach higher values, and to obtain stronger anisotropic effects due to nonlinear

interactions modified by rotation, new high-resolution ($128 \times 128 \times 512$) LES runs were carried out for homogeneous rotating turbulence (Cambon, Mansour & Squires 1994, hereafter referred to as CMS). These computations used the same numerical procedure as Squires *et al.* (1993, 1994) with a Kraichnan-type subgrid-scale model including a Rossby number correction. The CMS results confirmed the anisotropic features of previous experimental, theoretical and DNS results in the intermediate range of Rossby numbers. These results were carefully analysed to ensure that the developed anisotropy was not due to boundary condition effects or other numerical artifacts. Consequently these databases will be used, rather than DNS results at low Reynolds number, in order to illustrate in a quantitative way the development of anisotropy indicators at high Reynolds number, and perform detailed comparisons with the 'EDQNM2' model of Cambon & Jacquin (1989). It is important to point out that the second threshold $Ro^{\omega} \sim 1$ characterized a reorganization rather than a 'freezing' of the anisotropy in CMS, but the behaviour for the largest elapsed times corresponding to $Ro^{\omega} < 1$ will not be discussed in the present paper, nor the quasi-asymptotic power laws addressed by Squires *et al.* (1993, 1994). For the same reason, the low-resolution (64^3) LES results by Bartello *et al.* (1994) will not be taken into account, since they involve even larger elapsed times, so that $Ro^{\omega} \ll 1$, with only a very few time-plots in the intermediate range of Rossby number, as far as we can tell from their paper. In order to avoid confusion, it is also worth noting that the Rossby number Ro, with no additional specification, is the macro-Rossby number in all the works quoted above, or $Ro = \epsilon/(2\Omega k) \sim Ro^{L}$, except in the paper of Bartello *et al.* (1994) in which $Ro = Ro^{\omega}$.

In addition to the range of parameters, it is important to discuss the way in which the initial three-dimensional isotropy is broken by nonlinear interactions modified by rotation, and how the anisotropic spectral shape is reflected by the classical anisotropy indicators in physical space, following the complete anisotropic description introduced by Cambon & Jacquin (1989) and used in CMS. As in other domains of geophysics, including quasi-geostrophic turbulence where rotation and stable stratification are simultaneously present, the long-time history can be considered as a transition towards the *slow manifold*. In the case of pure rotation, the slow manifold corresponds to two-dimensional modes (for which the dependency on the longitudinal – onto the rotation axis – space coordinate vanishes) or to the wave-plane normal to the rotation axis, in Fourier space. The rapidity of the transition may depend on the initial 'statistical measure' of this slow manifold. For instance, this measure is zero in the isotropic case (where tridimensionality is maximum from a statistical point of view), and the transition may involve very long times, unreachable by current experiments or DNS. On the other hand, this transition can be dramatically accelerated if significant two-dimensional contributions to the velocity field are initially present, as some germs of two-dimensionality. The effect of initially two-dimensional modes on the low-wavenumber range was extensively investigated by Dang & Roy (1985), and Teissèdre & Dang (1987) using DNS. Their results on stabilization of two-dimensional eddies can be interpreted as showing only that rotation inhibits the energy cascade, so that the two-dimensional – large-scale – contribution is more and more dominant since the three-dimensional – small scale – contribution is dissipated. This dissipation is due to the fact that the energy drain from larger scales is cut by rotation. A similar problem was also addressed by Bartello *et al.* (1994) using LES. They argued that because of the presence of an inverse energy cascade, the energy cascade is no longer inhibited but enhanced. Our qualitative argument is as follows: the inverse energy cascade is generated by the resonant triads for very small Ro. However, when Ro

is not too small, these triads are diluted in the non-resonant ones, which themselves reduce the energy transfer, whereby they damp almost all possibility of an inverse cascade occurring. Ultimately, the reduction of the energy cascade by rotation is attributed to a reduction of energy transfer, due to the scrambling of non-resonant triads in the triple correlations of the fluctuating velocity. In physical space, we will show that the damping of the skewness is a by-product of this effect.

In this paper we shall survey previous works, which are summarized, and we shall demonstrate that the reported results are self-consistent, and present new quantitative results useful for the subsequent statistical modelling of actual rotating flows.

Section 2 is devoted to basic equations and what can be understood from pure linear or weakly nonlinear theoretical approaches, from a pure dynamical point of view. For convenience the EDQNM models, and especially the most sophisticated version 'EDQNM2', are introduced in this section in order to underline the important common background that they share with the theories of wave turbulence.

The corpus of agreed statements about the statistics of rotating homogeneous turbulence is presented in §3, including both numerical and experimental results. Energy cascade is studied using isotropically accumulated quantities, with application to K–ϵ modelling.

Section 4 is devoted to a detailed analysis of anisotropic features. The analysis is based on a stringent relationship between the anisotropy indicators in physical space (single-point correlations) and the underlying spectral structure. The development of several anisotropy indicators obtained from the recent CMS database are compared with that calculated using the EDQNM2. A recap of results and open problems is given in §5.

2. Basic equations and approach to wave turbulence

In the absence of mean gradients and external forces, the starting point of the dynamical study is the Navier–Stokes equation in a rotating frame of reference

$$u_{i,t} + 2\epsilon_{ijl}\Omega_j u_l - \nu\nabla^2 u_i + (p^r/\rho)_{,i} = -(p^s/\rho)_{,i} - u_j u_{i,j} \tag{2.1}$$

where $u_i(\boldsymbol{x}, t)$ is the velocity field, p^r and p^s are the rapid and the slow pressure fields associated with the linear and nonlinear terms respectively, ϵ_{ijl} the third-order alternating tensor, Ω_i the angular velocity of the rotating frame, and ν the kinematic viscosity. For convenience, the nonlinear terms are placed on the right-hand side of the equation. The fluid is considered to be incompressible, so that the velocity field is solenoidal (divergence free) $u_{i,i} = 0$, the density ρ is constant, and the pressure is governed by a Poisson equation that includes both a linear term with respect to u_i (p^r) – the divergence of the Coriolis force, and a nonlinear one (p^s) – the divergence of the convective term. The pressure can be removed from consideration by taking the curl of equation (2.1). This operation yields the following vorticity equation:

$$\omega_{i,t} - 2\Omega_j u_{i,j} + \nu\nabla^2\omega_i = -u_j\omega_{i,j} + u_{i,j}\omega_j \tag{2.2}$$

where the 'vortex-stretching' term $u_{i,j}(2\Omega_j + \omega_j)$, which involves the absolute vorticity $2\Omega_j + \omega_j$, is split in order to collect the nonlinear terms on the right-hand side. To close the vorticity equation, in terms of ω_i, the velocity is obtained by solving the equation

$$\nabla^2 u_i = -\epsilon_{ijl}\omega_{l,j}.$$

In both cases (equations (2.1) and (2.2)) the solution to a Poisson equation is needed even after splitting the equations in terms of linear and nonlinear effects and solving the linearized equations. This requirement, and the fact that at small Rossby numbers plane waves of the form $\exp(\mathrm{i}(k_j x_j \pm \sigma t))$ are solutions to the linearized equations, motivate the decomposition of the flow field into Fourier modes, as will be apparent in what follows.

Investigations of both linear and – even weakly – nonlinear terms were carried out to explain the first phase of the transition from a three-dimensional state to a two-dimensional one. The classic argument used to explain such a bidimensionalization, known as the Proudman theorem (Proudman 1916; Taylor 1921), is based on the fact that both the nonlinear and the viscous terms in (2.2) can be neglected given a very small Rossby number and a very high Reynolds number. However, this level of approximation yields a pure linear inviscid regime where energy, helicity and enstrophy spectra are conserved. In this case, any transition to a two-dimensional state is excluded. In order to include the two-dimensional condition ($\Omega_j u_{i,j} = 0$; no spatial derivative along the direction of the external angular velocity vector), the time derivative, in the linearized inviscid equations, is neglected given a long-time assumption. It is important to point out that the scaling of the vorticity time derivative is an assumption, and it cannot be related *a priori* to the true nonlinear dynamics, which is removed from consideration in the strict zero Rossby number limit. In the absence of geometrical constraints (walls, thin layer), this scaling is justified only if an external timescale is present (for instance pushing a ball slowly in the Taylor rotating tank); even if a rescaling of the time can take into account the nonlinear dynamics in other cases, such as in spherically compressed flows (see Zimont & Sabel'nikov 1975; Cambon, Mao & Jeandel 1992*b*), there is no such simple and stringent argument in rotating flows. In other words, the Proudman theorem strictly shows that the 'slow manifold' (limit of vanishing $\omega_{i,t}$) is the two-dimensional manifold, but it does not prove transition toward the two-dimensional state, which is a nonlinear phenomenon. Hence an explicit investigation of nonlinear terms is required for the purpose of studying the transition towards the slow – or two-dimensional – manifold.

2.1. *The equations of motion in wave space*

Solutions of the linearized equations (2.1) or (2.2) are found in Fourier space in terms of the Fourier components, $\hat{u}_i$ or $\hat{\omega}_i$ defined as follows:

$$\hat{u}_i(\boldsymbol{k}, t) = \frac{1}{(2\pi)^3} \int u_i(\boldsymbol{x}, t) \exp(-\mathrm{i}\boldsymbol{x}\cdot\boldsymbol{k})\ \mathrm{d}^3\boldsymbol{x},$$

$$\hat{\omega}_i(\boldsymbol{k}, t) = \frac{1}{(2\pi)^3} \int \omega_i(\boldsymbol{x}, t) \exp(-\mathrm{i}\boldsymbol{x}\cdot\boldsymbol{k})\ \mathrm{d}^3\boldsymbol{x}.$$

Starting from the linearized equation in spectral space, in which the pressure is eliminated, it is possible to define an orthonormal basis of the linear operator eigenmodes for $\hat{u}$ or $\hat{\omega}$:

$$N_i(\epsilon\boldsymbol{k}) = e_i^2(\boldsymbol{k}) - \mathrm{i}\epsilon e_i^1(\boldsymbol{k})\ , \qquad \epsilon = +1, -1\ , \qquad \mathrm{i}^2 = -1 \tag{2.3}$$

where $\boldsymbol{e}^1, \boldsymbol{e}^2$ form a direct orthonormal frame in the plane normal to the wavevector $\boldsymbol{k}$, the so-called Craya–Herring frame (Craya 1958; Herring 1974). The two – complex conjugate – eigenmodes $N_i(\boldsymbol{k})$ and $N_i^*(\boldsymbol{k}) = N_i(-\boldsymbol{k})$ are defined as in Cambon & Jacquin (1989) who emphasized their orthonormal properties (conservation of frame-invariants and of the form of realizability constraints for covariances matrices in the

eigenframe) but the definitions by Greenspan (1968) or Waleffe are almost the same. In addition to being the eigenmodes of the linear regime for strong rotation, these are also the eigenmodes of the curl operator, i.e. $\epsilon_{ijl}\mathrm{i}k_l N_j(\boldsymbol{k}) = N_i(\boldsymbol{k})$, and are of interest even without rotation. Following Waleffe, they will be referred to as *helical modes* hereafter, and the sign ϵ (s_k in Waleffe) will be referred to as the *polarity*. Then the divergence-free velocity field in Fourier space is projected on the basis of helical modes:

$$\hat{u}_i = \xi_{-1} N_i(-\boldsymbol{k}) + \xi_{+1} N_i(\boldsymbol{k}) \tag{2.4}$$

or

$$\xi_\epsilon(\boldsymbol{k}, t) = \tfrac{1}{2}\hat{u}_i(\boldsymbol{k}, t) N_i(-\epsilon\boldsymbol{k}) \ , \qquad \epsilon = +1, -1, \tag{2.5}$$

and the basic equation (2.1) is rewritten in terms of the helical mode intensities, considering both linear and nonlinear terms, so that

$$\left[\frac{\partial}{\partial t} - \mathrm{i}\epsilon\frac{2\Omega_j k_j}{k} + \nu k^2\right] \xi_\epsilon(\boldsymbol{k}, t) = \sum_{\epsilon'\epsilon''} \int_{\boldsymbol{k}+\boldsymbol{p}+\boldsymbol{q}=0} M_{\epsilon\epsilon'\epsilon''}(\boldsymbol{k}, \boldsymbol{p}, \boldsymbol{q}) \xi^*_{\epsilon'}(\boldsymbol{p}, t) \xi^*_{\epsilon''}(\boldsymbol{q}, t) \ \mathrm{d}^3\boldsymbol{p} \tag{2.6}$$

(see Cambon & Jacquin 1989). In this equation, which is completely general, the – linear – left-hand-side term is diagonal, since the helical modes are eigenmodes of the linear regime, and the – nonlinear – term conserves the form of a triadic integral (as for the Fourier transform of the basic convective term $\widehat{u_j u_{i,j}}$) but involves a new 'influence matrix', a symmetrized form in $\boldsymbol{p}$ and $\boldsymbol{q}$, which reads

$$M_{\epsilon\epsilon'\epsilon''} = -\tfrac{1}{4}\mathrm{i}\, k_l \left[N_l(\epsilon'\boldsymbol{p}) N_i(\epsilon\boldsymbol{k}) N_i(\epsilon''\boldsymbol{q}) + N_l(\epsilon''\boldsymbol{q}) N_i(\epsilon\boldsymbol{k}) N_i(\epsilon'\boldsymbol{p})\right] \ . \tag{2.7}$$

A slightly different form can be found starting from $\omega \times \boldsymbol{u}$ (Waleffe), instead of $\boldsymbol{u}\cdot\nabla\boldsymbol{u}$, for the nonlinear term in (2.1):

$$M_{\epsilon\epsilon'\epsilon''} = \tfrac{1}{4}\mathrm{i}\boldsymbol{N}(\epsilon\boldsymbol{k}) \cdot \left[\left(\boldsymbol{p} \times \boldsymbol{N}(\epsilon'\boldsymbol{p})\right) \times \boldsymbol{N}(\epsilon''\boldsymbol{q}) + \left(\boldsymbol{q} \times \boldsymbol{N}(\epsilon''\boldsymbol{q})\right) \times \boldsymbol{N}(\epsilon'\boldsymbol{p})\right] \ . \tag{2.8}$$

Of course, equation (2.6) can be derived from the vorticity equation (2.2), in agreement with

$$\hat{\omega}_i = k\left[\xi_{+1} N_i(\boldsymbol{k}) - \xi_{-1} N_i(-\boldsymbol{k})\right].$$

If the nonlinear and viscous terms are ignored in (2.6), the simple exponential solutions exhibit the dispersion law of the inertial waves $\sigma = 2\Omega_j k_j/k = 2\Omega k_3/k$ (with $\Omega_i = \Omega\delta_{i3}$ from now on, without loss of generality). The time dependence vanishes only for $k_3 = 0$, so that the wave-plane $k_3 = 0$ can be referred to as the *slow manifold*, according to classic works in geophysics (Lorenz 1980; Hasselman 1962). The slow manifold coincides with the geostrophic mode in the case of pure rotation, so that a tendency towards bidimensionalization (which cannot be demonstrated in the pure linear regime) would be a concentration towards the 'slow manifold'. Such a tendency can be studied at low Rossby number using the following new – and final – change of variables

$$\left.\begin{aligned} \xi_\epsilon(\boldsymbol{k}, t) &= a_\epsilon(\boldsymbol{k}, T) \exp(2\mathrm{i}\epsilon\Omega t k_3/k - \nu k^2 t) \ , \\ \xi_{\epsilon'}(\boldsymbol{p}, t) &= a_{\epsilon'}(\boldsymbol{p}, T) \exp(2\mathrm{i}\epsilon'\Omega t p_3/p - \nu p^2 t) \ , \\ \xi_{\epsilon''}(\boldsymbol{q}, t) &= a_{\epsilon''}(\boldsymbol{q}, T) \exp(2\mathrm{i}\epsilon''\Omega t q_3/q - \nu q^2 t) \ . \end{aligned}\right\} \tag{2.9}$$

The equations of motion in terms of a_ϵ are then given as

$$\begin{aligned} \frac{\partial}{\partial t} a_\epsilon(\boldsymbol{k}, T) = {} & \textstyle\sum_{\epsilon'\epsilon''} \int_{\boldsymbol{k}+\boldsymbol{p}+\boldsymbol{q}=0} M_{\epsilon\epsilon'\epsilon''}(\boldsymbol{k}, \boldsymbol{p}, \boldsymbol{q}) a^*_{\epsilon'}(\boldsymbol{p}, t) a^*_{\epsilon''}(\boldsymbol{q}, t) \\ & \times \exp\left[-2\mathrm{i}\Omega t(\epsilon k_3/k + \epsilon' p_3/p + \epsilon'' q_3/q)\right] \exp\left[-\nu(q^2 + p^2 - k^2)t\right] \ \mathrm{d}^3\boldsymbol{p}. \end{aligned} \tag{2.10}$$

This last equation is almost the same as (2.6), but it no longer contains the linear 'Coriolis' term on the left-hand side and the influence matrix on the right-hand side is weighted by the following 'triadic' wave factor:

$$\exp\left[2\mathrm{i}\Omega t(\epsilon k_3/k + \epsilon' p_3/p + \epsilon'' q_3/q)\right]. \tag{2.11}$$

Equations (2.9) and (2.10) are valid in terms of the single time ($t = T$ in a_ϵ). Thus the introduction of a slow timescale $T = Ro \times t$ with Ro a small formal parameter similar to a Rossby number allows further investigation as follows. Non-resonant triads lead to a rapid scrambling of nonlinearity for large Ωt. Hence, since the non-resonant triads average out over the long timescale, it can be shown (Benney & Saffman 1966; Waleffe) that at the lowest order of the Rossby number, the slow dynamics is governed only by resonant triads

$$\epsilon k_3/k + \epsilon' p_3/p + \epsilon'' q_3/q = 0 \tag{2.12}$$

such that the wave factor (2.11) is 1 in (2.10). In this case, the rotation Ω drops out of the equations governing the evolution of a_ϵ, and the interactions are the same as in the non-rotating case. This implies that the slow time T scales with the turbulence time, and not the rotation.

The dynamics of the energy and the helicity at a given wavenumber,

$$e = \tfrac{1}{2}\hat{u}_i^*\hat{u}_i = \xi_{+1}^*\xi_{+1} + \xi_{-1}^*\xi_{-1} = a_{+1}^* a_{+1} + a_{-1}^* a_{-1}, \tag{2.13}$$

$$h = \tfrac{1}{2}\hat{u}_i^*\hat{\omega}_i = k(a_{+1}^* a_{+1} - a_{-1}^* a_{-1}), \tag{2.14}$$

can be derived from the exact equation (2.6). In the presence of strong rotation these equations are almost the same as without rotation, *but the triads involved in the nonlinear terms are restricted to resonant triads. A priori*, the low Rossby number limit does not yield separation of the rapid inertial wavy modes from the slow two-dimensional modes (both are slow in terms of their energy), but yields a separation between the resonant triads which drive the slow dynamics and the non-resonant triads for which the nonlinear dynamics are damped. In order to predict a transition towards a two-dimensional state on a slow timescale, it is necessary

(*a*) to show that the resonant triads do tend to concentrate the spectral energy density towards the two-dimensional wave-plane $k_3 = 0$ (the slow manifold);

(*b*) then, to give a statistical meaning to 'slow' time and 'low' Rossby number: since the measure of the manifold of almost resonant triads (given a broadening of the resonant condition $(\epsilon k_3/k + \epsilon' p_3/p + \epsilon'' q_3/q) = O(Ro)$) is very small at very small Rossby number, the related spectral transfer terms may not be high enough for the transition to be triggered in a physically reachable elapsed time. This problem is particularly relevant when starting with a three-dimensional isotropic state where the measure of the two-dimensional slow manifold is zero. If the state is closer to a two-dimensional one, a two-dimensional dynamics with inverse cascade can accelerate the transition.

Note that these issues about transition to a two-dimensional state are very different (despite apparent analogies) from quasi-geostrophic flows where stable stratification is present, since the slow manifold (vortex and not wavy modes) has an important measure even in three-dimensional isotropic turbulence, and in MHD flows at low magnetic Reynolds number, where the transition can be predicted in the pure linear limit, through a non-isotropic linear Joule dissipation term (Cambon & Godeferd 1993; Godeferd & Cambon 1994).

2.2. *Two-point correlations*

The equations governing the evolution of the two-point correlations are needed to quantify the effects of rotation on the turbulence statistics. These can be derived by first expressing the second-order spectral tensor (covariance matrix of $\hat{u}_i$) in terms of new variables (Cambon & Jacquin 1989),

$$\hat{U}_{ij}(\boldsymbol{k},t) = e(\boldsymbol{k},t)P_{ij}(\boldsymbol{k}) + \mathrm{Re}\left[Z(\boldsymbol{k},t)N_i(\boldsymbol{k})N_j(\boldsymbol{k})\right] + \mathrm{i}\epsilon_{ijl}\frac{k_l}{k}\frac{h(\boldsymbol{k},t)}{k}, \tag{2.15}$$

where $P_{ij} = \delta_{ij} - k_i k_j/k^2$, also equal to the symmetric part of $N_i N_j^*$, is the classic solenoidal projector. The cross-term $Z = 2\xi_{-1}^*\xi_{+1}$, represents a *polarization anisotropy*. The above equation is valid for any anisotropic configuration; it generalizes and/or simplifies previous formalisms by Batchelor (1953) and Craya (1958) for homogeneous incompressible turbulence.

It is clear from (2.15) that we need only the three terms e, Z and h (e, $|Z|$ and h are the invariants) of the spectral tensor $\hat{U}_{ij}$ to describe all of the quadratic correlations. The starting point of analyses by both Cambon & Jacquin (1989) and Waleffe (1991) is the following exact system of equations for the invariants in terms of the helical modes intensities:

$$\left.\begin{aligned}\left[\frac{\partial}{\partial t} + 2\nu k^2\right] e &= T^e,\\ \left[\frac{\partial}{\partial t} + 2\nu k^2 + 4\mathrm{i}\Omega\frac{k_3}{k}\right] Z &= T^z,\\ \left[\frac{\partial}{\partial t} + 2\nu k^2\right] h &= T^h,\end{aligned}\right\} \tag{2.16}$$

in addition to the set of terms in (2.13), (2.14). Cubic terms T^e and T^h were investigated by Waleffe (1991) before using any statistical averaging and any closure, whereas the EDQNM2 model by Cambon & Jacquin concerned T^e and T^z. It is worth noting that the complete set e, Z, h is needed for expressing the velocity or vorticity covariances matrices related to any homogeneous anisotropic flow. The helicity is needed for flows with initial helicity.

The previous discussions were for the general case of homogeneous flows. In what follows, we shall concern ourselves with the statistics of the flow. To simplify the notation, we shall use e, Z, h, T^e, T^z, T^h to refer to statistically averaged quantities, for instance $\frac{1}{2}\langle\hat{u}_i^*(\boldsymbol{p},t)\hat{u}_i(\boldsymbol{k},t)\rangle = e(\boldsymbol{k},t)\delta(\boldsymbol{k}-\boldsymbol{p})$ instead of $e = \frac{1}{2}\hat{u}_i^*\hat{u}_i$. From the definitions (2.13), (2.14) with or without statistical averaging, a non-dimensional helicity ratio, always smaller than 1, can be defined as $h/(ke)$, whereas the non-dimensional correlation coefficient between ξ_{+1} and ξ_{-1} is

$$C(\xi_{+1},\xi_{-1}) = \frac{\langle\xi_{-1}^*\xi_{+1}\rangle}{(\langle\xi_{+1}^*\xi_{+1}\rangle\langle\xi_{-1}^*\xi_{-1}\rangle)^{1/2}} = \frac{Z}{(e^2-(h/k)^2)^{1/2}}. \tag{2.17}$$

The above complex ratio, whose modulus is an invariant smaller than or equal to 1, characterizes a polarization anisotropy and plays an essential role in any configuration of homogeneous anisotropic turbulence, and especially in the case of pure rotation.

The EDQNM2 model of Cambon & Jacquin (1989) for T^e and T^z dealt with both items (*a*) and (*b*) mentioned in §2.1. This model which is summarized in the next section and the Appendix, could be derived from a classic EDQNM model for triple correlations in terms of a_ϵ starting from the exact equations (2.10); it allowed interpolation from the wave turbulence at low Rossby number, because of its

consistency with the resonant condition, to high Rossby number turbulence, where it meets the conventional EDQNM model (Orszag 1970; André & Lesieur 1978). The model was numerically solved as a 'black box' but the simpler and more elegant arguments given by Waleffe for item (*a*) using his 'triad instability principle' will be summarized in §2.4.

2.3. *EDQNM models*

The EDQNM-type models can be introduced and constructed using different approaches (two-point closures for triple correlations, stochastic models) and they are often developed and applied only in the case of isotropic and 'strong' turbulence. The EDQNM procedure yields a closure for third-order velocity correlations at two points (those involved in the transfer terms on the right-hand sides of (2.16)) in terms of second-order velocity correlations at two points (the e, Z, h set in the general case). In this sense, EDQNM is a triple-order two-point closure model, where the 'two-point' aspect is addressed using spectral space for mathematical convenience. Accordingly, the specific closure problem coming from the expression of pressure–velocity gradient or dissipation terms in second-order single-point closure models, due to non-local operators, is avoided. The only closure problem comes from the generalized transfer terms (T^e, T^z, T^h) which reflect the nonlinearity, so that the system of equations (2.16) reproduces RDT for vanishing right-hand sides. The mathematical structure of these 'two-point closure models' comes from the expression of fourth-order correlations, which are involved in the rate equations for triple correlations, in terms of products of double correlations as for a normal law (quasi-normal approximation). Doing that, the role of fourth-order cumulants is formally ignored, and it is restored through the addition of a linear relaxation of triple correlations by means of an 'eddy damping' term. Finally the Markovian assumption amounts to truncating the self-memory of triple correlations, in order to find a simpler and more reliable instantaneous – but non-local – closure relationship of triple in terms of double correlations. It is important to point out that the mathematical structure is given by the 'QNM' part of the theory, whereas only a scalar eddy-damping coefficient needs an *ad hoc* adjustment.

In what follows we shall review two versions of the EDQNM model, which will be compared to results from DNS or LES data. In the simpler one (Cambon, Bertoglio & Jeandel 1981), called EDQNM hereafter, the structure of a basic model for isotropic turbulence (see Orszag 1970) is conserved and the effect of rotation is taken into account in the eddy-damping coefficient (André & Lesieur 1978) only by replacing the enstrophy of the largest eddies $\langle\omega^2\rangle^{<k} = 2\int_0^k p^2 E(p,t)\mathrm{d}p$ by the *absolute enstrophy* of the largest eddies $\langle\omega^2\rangle^{<k} + 4\Omega^2$, so that the eddy-damping term η present in the characteristic time θ_{kpq} of triple correlations is

$$\left.\begin{aligned} \eta^{\Omega}(k,t) &= \nu k^2 + \tfrac{1}{2}A(\langle\omega^2\rangle^{<k} + 4\Omega^2)^{1/2}, \\ \langle\omega^2\rangle^{<k} = 2\int_0^k p^2 E(p,t)\mathrm{d}p, \quad \theta_{kpq} &= \frac{1}{\eta^{\Omega}(k,t) + \eta^{\Omega}(p,t) + \eta^{\Omega}(q,t)}. \end{aligned}\right\} \tag{2.18}$$

This correction was proposed on the grounds of a literal interpretation of the eddy-damping coefficient based on $\langle\omega^2\rangle^{<k}$ as the 'turn-over time' of the largest eddies. The value of the unique constant $A = 0.366$ is kept the same as in the isotropic non-rotating case. The isotropic structure implies $e = E(k,t)/(4\pi k^2)$, $Z = h = 0$, $T^e = T(k,t)/4\pi k^2$, $T^z = T^h = 0$, so that the classic, i.e. isotropically accumulated by

integration of T^e over the angular dependent variables, energy transfer is given by

$$T(k,t) = \int_{\Delta_k} \theta_{kpq}(t) S^{QN}(k,p,q,t) \mathrm{d}p\mathrm{d}q \tag{2.19}$$

where the superscript QN is for a quasi-normal expression, denoted S^{QN}, which is proportional to $E(q,t)[k^2E(p,t) - p^2E(k,t)]$. The detailed form of S^{QN}, and $T(k,t)$, is cumbersome, and is presented in the Appendix for completeness.

The more advanced version, called EDQNM2 (Cambon 1982; Cambon & Jacquin 1989) reflects more accurately the wave dynamics and is capable of taking into account the anisotropic features. We find that only the EDQNM2 model for closing the spectral transfer terms T^e and T^Z was capable of predicting all the anisotropic features observed in the DNS and LES results and it provides a synoptic scheme to interpret and reconcile the various and apparently contradictory trends shown by results from experiment and DNS. In addition to their symbolic abridged form (Cambon & Jacquin 1989), the detailed equations have only been written in internal reports and in Jacquin's thesis, with some remaining typographical errors, so that they are rewritten in the Appendix, where the interested reader could find a lot of analogies with the formalism developed and published by Waleffe. Starting from the exact equations (2.6) and (2.8), it is possible to write the rate equation for triple correlation terms $\langle a_\epsilon(\boldsymbol{k},t) a_{\epsilon'}(\boldsymbol{p},t) a_{\epsilon''}(\boldsymbol{q},t)\rangle$ and to close it by the conventional eddy-damped quasi-normal technique. In doing so, the model equations for the generalized transfer terms T^e, T^z in (2.16) involve sums of eight contributions (according to polarities of triads, as also shown by Waleffe), and these contribution are weighted by the rotation-dependent factor in (2.11),

$$T^e = \sum_{\epsilon,\epsilon',\epsilon''=-1,+1} \int_{\boldsymbol{k}+\boldsymbol{p}+\boldsymbol{q}=0} \frac{S^{e(QN)}(\epsilon\boldsymbol{k}, \epsilon'\boldsymbol{p}, \epsilon''\boldsymbol{q}, t)}{\theta_{kpq}^{-1} + 2\mathrm{i}\Omega(\epsilon k_3/k + \epsilon' p_3/p + \epsilon'' q_3/q)} \mathrm{d}^3\boldsymbol{p} \tag{2.20}$$

with a similar equation for T^z. The numerator of the integrand takes into account the quasi-normal expansion for non-isotropic turbulence and is closed in terms of e and Z, whereas the denominator involves viscous and eddy-damping effects through θ_{kpq}, and explicit 'linear' rotation effects on triple correlation through the phase of the term in (2.11). In effect, the classic timescale θ_{kpq} in the isotropic non-rotating case is replaced by the following triadic complex timescales:

$$\theta_{kpq}^{\epsilon\epsilon'\epsilon''} = \frac{\theta_{kpq}}{1 + 2\mathrm{i}\theta_{kpq}\Omega(\epsilon k_3/k + \epsilon' p_3/p + \epsilon'' q_3/q)}. \tag{2.21}$$

The above expression is consistent with 'wave turbulence' results which show no explicit rotation effects for the resonance condition. In addition, the quasi-normal assumption is supported at low Rossby number by the 'wave-turbulence' analysis of Benney & Saffman (1966). The possible broadening of the resonance condition depends on the order of magnitude of the 'triadic Rossby number' $1/(2\theta_{kpq}\Omega)$ in (2.21). Only the choice of the *ad hoc* damping coefficient makes reference to 'strong' developed turbulence, and allows a matching with the behaviour at high Rossby number. Of course the EDQNM model corrected for rotation, using (2.18) and (2.19), can be seen as a simplified model for T, that is the spherically accumulated contribution of T^e. It is hoped that these model equations, and not only the use of the related numerical code as a black box, will help to investigate the role of the 'polarization transfer' T^z in the two-dimensional manifold $k_3 = 0$, a role which cannot be elucidated from the more recent analyses by Waleffe or Squires *et al.* (1994), but

is the key for understanding the most striking anisotropic feature, i.e. the de-coupling of the two integral lengthscales with vertical separation. These equations are solved using the simplifications for a semi-axisymmetric configuration without helicity, which is the simplest anisotropic statistical configuration consistent with the basic equations, and is created starting from a pure three-dimensional isotropic case.

2.4. *Simplified triad interactions*

The principle of triad instability was stated by Waleffe in the non-rotating case ($\xi_\epsilon = a_\epsilon$), looking at a single triad in terms of the helical modes in (2.6) or (2.10), so that

$$\left.\begin{aligned} a_\epsilon(\boldsymbol{k},t)_{,t} &= (\epsilon' p - \epsilon'' q)K a^*_{\epsilon'}(\boldsymbol{p},t)a^*_{\epsilon''}(\boldsymbol{q},t), \\ a_{\epsilon'}(\boldsymbol{p},t)_{,t} &= (\epsilon'' q - \epsilon k)K a^*_{\epsilon''}(\boldsymbol{q},t)a^*_{\epsilon}(\boldsymbol{k},t), \\ a_{\epsilon''}(\boldsymbol{q},t)_{,t} &= (\epsilon k - \epsilon' p)K a^*_{\epsilon}(\boldsymbol{k},t)a^*_{\epsilon'}(\boldsymbol{p},t). \end{aligned}\right\} \tag{2.22}$$

Starting from (2.8), the factor K is expressed as

$$\begin{aligned} K &= -\tfrac{1}{4}\left(\boldsymbol{N}^*(\epsilon\boldsymbol{k}) \times \boldsymbol{N}^*(\epsilon'\boldsymbol{p})\right) \cdot \boldsymbol{N}(\epsilon''\boldsymbol{q}) \\ &= \mathrm{e}^{\mathrm{i}(\epsilon\lambda+\epsilon'\lambda'+\epsilon''\lambda'')}\frac{\epsilon\epsilon'\epsilon''}{8kpq}(2k^2p^2 + 2p^2q^2 + 2q^2k^2 - k^4 - p^4 - q^4)^{1/2}\,. \end{aligned} \tag{2.23}$$

The main advantage of the decomposition in terms of helical modes is that the 'influence matrix' in (2.7) or (2.8) is the product of a very simple term, including only the *moduli* of the triad vectors, and a factor completely symmetric in terms of $\epsilon\boldsymbol{k}$, $\epsilon'\boldsymbol{p}$, $\epsilon''\boldsymbol{q}$ namely $\exp(\mathrm{i}(\epsilon\lambda + \epsilon'\lambda' + \epsilon''\lambda''))$ above, which concentrates all the angular dependency (see also Cambon & Jacquin 1989 and the Appendix). The above system (2.22) has a strong analogy with the stability of the rotating motion of a solid body around the three principal axes of the inertial ellipsoid, with the lengths of the sides of the triangle (k, p, q) playing the role of principal inertia coefficients. Assuming that the most unstable mode (in the sense of the classic stability analysis of the above system) transfers energy to the two others, the direction of energy transfers is predicted for any geometry (the orientation need not be prescribed) of a triad of helical modes, at given polarities ϵ, ϵ',ϵ''. The direction of the transfer depends on the sign of the coefficients in the above three equations (2.22), and thus can be related to the values of the polarity indices if an ordering, e.g. $k > p > q$, is assumed. A similar argument can be found in Pedlosky (1986). In the presence of strong rotation, the principle of triad instability is unchanged, but the analysis is restricted to resonant triads only, i.e. for $\epsilon\cos\theta_k + \epsilon'\cos\theta_p + \epsilon''\cos\theta_q = 0$. In this case, the geometrical factors relating the orientations of $\boldsymbol{k}$, $\boldsymbol{p}$ and $\boldsymbol{q}$, given by their cosines $\cos\theta_k = k_3/k$, $\cos\theta_p = p_3/p$ and $\cos\theta_q = q_3/q$, have been shown by Waleffe to be such that the transfer of energy always goes from a less slanted leg of the triad (with respect to the rotation vector) to a more slanted one, when the instability principle holds, according to the equations

$$\frac{\cos\theta_k}{(\epsilon' q - \epsilon'' p)} = \frac{\cos\theta_p}{(\epsilon'' k - \epsilon q)} = \frac{\cos\theta_q}{(\epsilon p - \epsilon' k)}\ ;$$

whence a drain of energy towards the direction orthogonal to $\boldsymbol{\Omega}$. Waleffe, however, points out that the rate of energy transfer vanishes exactly when the wavevector $\boldsymbol{k}$ reaches the equatorial orientation.

In the presence of strong rotation, it is sufficient to restrict the analysis to resonant triads, to show that the simultaneous conditions given by the 'triad instability principle' on the geometry and the resonance condition predict an angular transfer towards

the waveplane normal to the rotation axis. Hence the analysis of wave turbulence at low Rossby number directly shows that the spectral density of energy tends to concentrate in the slow manifold $k_3 = 0$. Nevertheless, Waleffe's analysis cannot provide quantitative measures of the effects of rotation on the turbulence statistics. In addition, the analysis does not give access to the polarization anisotropy (2.17), which is a key parameter when looking at the detailed anisotropic features observed in both Reynolds stresses and the integral lengthscales.

3. The effects of rotation on the turbulence statistics

There exists in the literature a wide consensus that rotation inhibits direct energy cascade in three-dimensional turbulence, so that the dissipation rate is reduced. Looking at the spherically averaged energy spectrum $E(k,t)$ (integral of e over spherical shells), rotation can affect only the spectral transfer term $T(k,t)$ since the classic Lin equation for the energy spectrum is not explicitly modified by the Coriolis force:

$$\frac{\partial E(k,t)}{\partial t} = T(k,t) - 2\nu k^2 E(k,t). \tag{3.1}$$

Integration over k of the above equation gives $(q^2/2)_{,t} = -\varepsilon$ since T has zero integral, but integration after multiplication by $2\nu k^2$ shows that T – modified by rotation – can affect the dynamics of the dissipation rate $\varepsilon = \nu\langle\omega_i\omega_i\rangle$:

$$\varepsilon_{,t} = 2\nu\langle\omega_i\omega_j u_{i,j}\rangle - 2\nu^2\langle\omega_{i,j}\omega_{i,j}\rangle. \tag{3.2}$$

The first term on the right-hand side represents turbulent stretching of vorticity and is a production term. It relates to the nonlinear spectral transfer term through

$$\langle\omega_i\omega_j u_{i,j}\rangle = \int_0^\infty k^2 T(k,t)\,\mathrm{d}k. \tag{3.3}$$

The second term represents a destruction of ε by viscous linear effects, or $2\nu^2\langle\omega_{i,j}\omega_{i,j}\rangle = \int_0^\infty (2\nu k^2)^2 E(k,t)\mathrm{d}k$. Rotation could play an explicit role only in the 'enstrophy-production term', thus breaking the balance between production and destruction often assumed in simple q^2–ε models. Under suitable non-dimensionalization, the enstrophy-production term involves the velocity derivative skewness

$$S = \frac{6\sqrt{15}}{7}\nu\langle\omega_i\omega_j u_{i,j}\rangle\frac{(q^2/2)}{\varepsilon^2}\frac{1}{Re^{1/2}}. \tag{3.4}$$

The above expression reduces to $-\langle u_{1,1}^3\rangle/\langle u_{1,1}^2\rangle^{3/2}$ in isotropic turbulence. $Re = (q^2/2)^2/\nu\varepsilon$ is a Reynolds number, which can be considered as the macro-Reynolds number, assuming $L \sim q^3/\varepsilon$. In the same way, the enstrophy-destruction term (second term on the right-hand side of (3.2)) involves a non-dimensional parameter G which can be expressed in the following way:

$$G = \frac{3\sqrt{15}}{7}(2\nu^2\langle\omega_{i,j}\omega_{i,j}\rangle - C_2(Re)\frac{\epsilon^2}{q^2/2})\frac{q^2/2}{\varepsilon^2}\frac{1}{Re^{1/2}}\ .$$

The classic ε-equation is then recovered as

$$\varepsilon_{,t} = \left[\frac{7}{3\sqrt{15}}(S-G)Re^{1/2} - C_2\right]\frac{\varepsilon^2}{q^2/2}$$

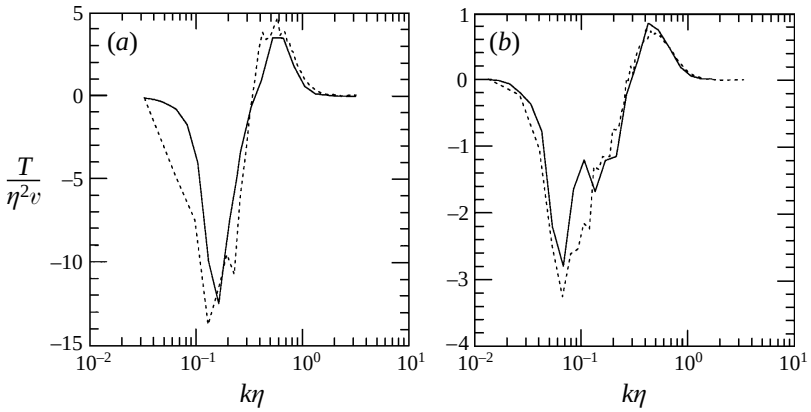

FIGURE 1. Energy transfer $T/(\eta^2 v)$ for: (*a*) ——— , EDQNM; and - - - - , 128^3 DNS. (*b*) ——— , EDQNM; and - - - - , 256^3 DNS.

where S is the only term which accounts for nonlinear dynamics directly affected by rotation (the contribution of triple contributions or spectral transfer, according to (3.3) and (3.4)), whereas G and C_2 reflect the viscous destruction term. As pointed out by Mansour *et al.* (1991*b*), G is the coefficient of the leading term in the expansion, in terms of Re, of the destruction term. The production–destruction equilibrium in isotropic (non-rotating) turbulence can be written very simply using S and G, since it amounts to $S = G$. A simple dynamic model for S and G, with a specified function $C_2(Re)$ was proposed by Mansour *et al.* (1991*b*), resulting in very good agreement with 128^3 and 256^3 DNS for large range of Rossby and Reynolds numbers. In what follows we shall compare the DNS results with EDQNM models (whose results were not quoted in the short paper by Mansour *et al.* 1991*b*); it is worth noticing that if a good model for T in (3.1), leading to a good model for S in (3.4) is provided, there is no need to provide a model for G, since the Lin equation is solved. Hence only DNS–EDQNM intercomparisons for S will be given in the following.

The non-rotating precomputations by Mansour *et al.* (1991*a*, *b*) were started with a classic narrow-band spectrum and run up to a time t_0 to build triple correlations (Mansour & Wray 1994). These precomputations were crucial for the study, as discussed in §2. They were needed to obtain a reliable power-law decay for the turbulent kinetic energy, and not only a plateau for the skewness S; this condition is more stringent (larger t_0) than in previous classic DNS, so that smaller Reynolds numbers are reached at the time $t = 0$ when the rotation is suddenly added. Nevertheless, only the long time precomputation ensures that the initial data are of physical relevance when the rotation is started. This precomputation also provided an opportunity to compare DNS and basic EDQNM in a quantitative way. For instance, the transfer term $T(k, 0)$ directly computed from the DNS data is compared to the one derived from the DNS energy spectrum $E(k, 0)$ through the EDQNM closure relation of type (2.19), for 128^3 and 256^3 in figures 1(*a*) and 1(*b*), respectively. The agreement is impressive, especially for the case with highest resolution (256^3); the results illustrate the advantage of the logarithmic step used in EDQNM for giving a better resolution of largest scales (smallest k), and justify keeping the constant A (see (2.18)), initially calculated at very high Reynolds number, unchanged for a very large range of Reynolds numbers.

The histories of the skewness are plotted in figure 2(*a*) for several rotation rates, and

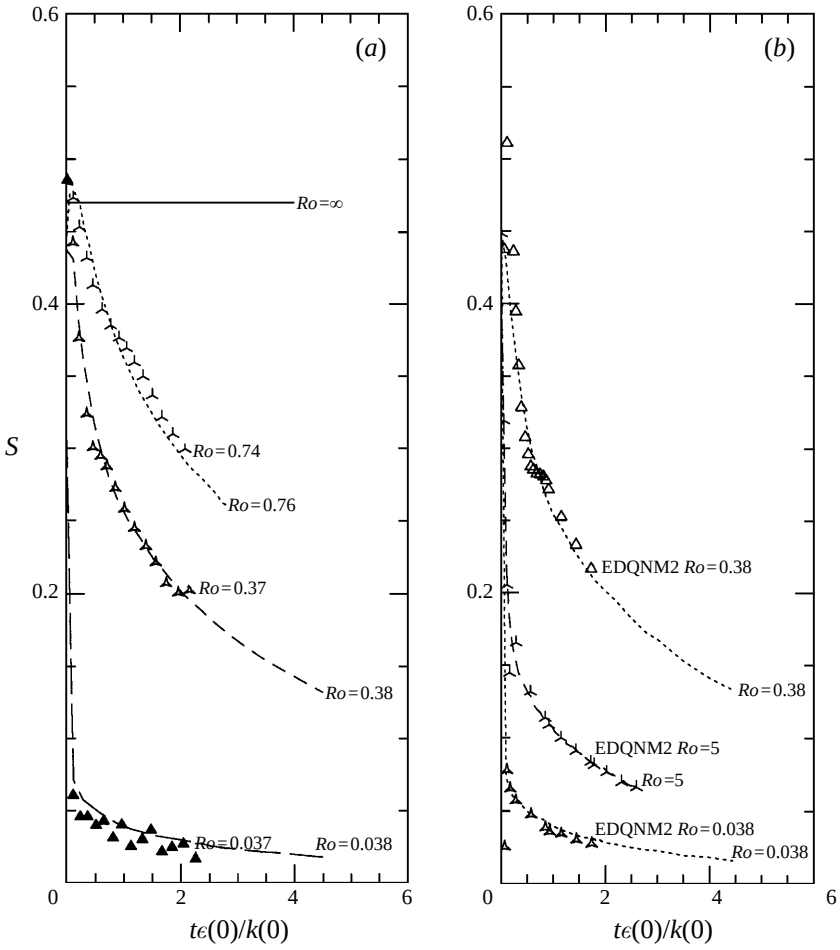

FIGURE 2. Evolution of skewness for the different indicated Rossby numbers given by (*a*) 128^3 DNS (symbols) and EDQNM (lines); (*b*) EDQNM2 (symbols) and EDQNM (lines).

the results from DNS are compared to the ones from the EDQNM model corrected for rotation started with the same energy spectrum $E(k,0)$ (3.1), (3.3), and (2.18). These results show strong damping of the skewness, which reflects the drop of triple correlations in the presence of rotation, and, again, the excellent agreement between DNS and EDQNM. The results of EDQNM2 and EDQNM are also compared in figure 2(*b*). These results confirm that a rough EDQNM model is sufficient for predicting the complex scrambling effects of rotation on triple correlations, when looking at spherically averaged quantities. However, only a model which takes into account the anisotropic effects of rotation in the nonlinear interactions (spectral transfer) can predict the anisotropic features, as discussed in the following section.

In order to collapse all of the results concerning the histories of the skewness, Mansour *et al.* (1991*b*) proposed plotting S versus the instantaneous Rossby number; a first attempt using the macro-Rossby Ro^L gave a good collapse for the plots at fixed initial Reynolds number (either 128^3 or 256^3) but a better overall collapse of all the data was found using a quantity proportional to the micro-Rossby number, or

$$Ro^\omega = \omega'/(2\Omega) = Ro^L(Re^L)^{1/2} = \sqrt{15}Ro^\lambda$$

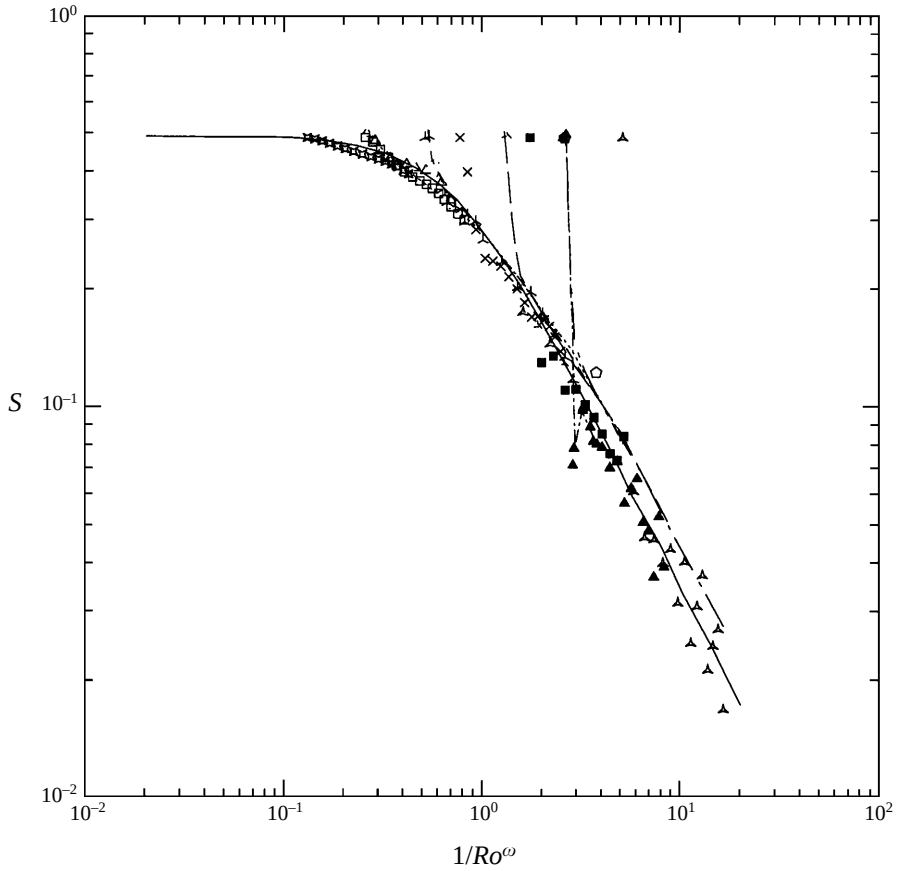

FIGURE 3. Variation of the skewness with respect to the inverse of the Rossby number Ro^ω. Curves show the EDQNM results, and symbols indicate (128^3 and 256^3) DNS computations; ——— , the analytical profile of (3.5); other lines represent particular EDQNM runs with initial low Rossby number.

where Ro^L and Re^L were evaluated by $\varepsilon/(2\Omega(\overline{q^2}/2))$ and $(\overline{q^2}/2)^2/(\nu\varepsilon)$ respectively. As shown in figure 3, all the runs for S histories start with the same initial value (close to 0.49), but eventually S tends to collapse on an unique curve $S = S^e(Ro^\omega)$. Guided by the good predictions of the basic EDQNM model, (2.18) suggests that the effects of rotation be of the form $[1 + (2\Omega)^2/\langle\omega^2\rangle^{<k}]^{-1/2}$ through the following equation:

$$S^e(Ro^\omega) = \frac{0.49}{[1 + 2/(Ro^\omega)^2]^{1/2}} \tag{3.5}$$

which is shown to fit very well the DNS and EDQNM data (see also figure 3). The above equation is consistent with a damping of nonlinear terms at a micro-Rossby number smaller than 1, so that a pure viscous decay ($T = 0$ in (3.1)) is recovered at small micro-Rossby number, as obtained by Speziale *et al.* (1987). The value 0.49 recovered at infinite Rossby number (no rotation) for the skewness is a classical result of the isotropic EDQNM model, and is in agreement with the DNS data. Corrections in terms of the Rossby number were proposed in the left-hand side of the dissipation rate equation (3.2), of the kind $C_{\epsilon 2}(Ro)(q^2/2)/\epsilon$, by Bardina *et al.* (1984) and Aupoix (1984) (see also Cambon, Jacquin & Lubrano 1992*a*), but these models

did not account for the separate and dynamically significant role of the production and destruction of the dissipation rate.

4. Spectral approach to anisotropic features: dimensionality and polarization

4.1. *Background: experimental evidence*

It is clear that nonlinear interactions modified by rotation trigger the onset of anisotropy. This nonlinearity makes the prediction of the onset of anisotropy difficult. Both the way in which the anisotropy is reflected by the usual indicators, and the first phase of reduction in dimensionality require a detailed two-point (or spectral with angular dependence) approach. A first insight to this problem was given by the DNS calculations of Bardina *et al.* (1985), who showed that anisotropy is primarily reflected by the integral lengthscales whereas the Reynolds stress tensor remained quasi-spherical, but the underlying anisotropic spectral shape and the relevant parameter regime were hardly discussed. The theoretical and experimental approach by Jacquin *et al.* (1989, 1990), and Cambon & Jacquin (1989), using mainly a non-isotropic spectral description, went further into characterizing the key anisotropy indicators and the parameter ranges. The main result of the experimental approach is that the most relevant anisotropy indicators involve the integral lengthscales with longitudinal (along the rotation axis) separation (index 3) but relative to either transverse L^3_{11} or longitudinal L^3_{33} velocity components, where

$$L^k_{ij} = \int_0^\infty \langle u_i(\boldsymbol{x}) u_j(\boldsymbol{x} + r\boldsymbol{n}^{(k)})\rangle \mathrm{d}r / \langle u_i(\boldsymbol{x}) u_j(\boldsymbol{x})\rangle \tag{4.1}$$

with $\boldsymbol{n}^{(k)}$ the unit vector along the direction axis x_k. They also showed that the anisotropy is triggered as soon as a macro-Rossby number becomes smaller than 1, provided the Reynolds number is high enough. More accurately, the quantities chosen for an optimal collapse of experimental data were the following.

(i) A longitudinal and a transverse macro-Rossby number

$$Ro_v = \frac{\langle u_3^2\rangle^{1/2}}{2\Omega L^3_{33}}\,, \qquad Ro_h = \frac{\langle u_1^2\rangle^{1/2}}{4\Omega L^3_{11}} \tag{4.2}$$

(these are equal in isotropic turbulence). The subscripts v (for longitudinal) and h (for transverse) refer to *vertical* (the axis of rotation) and *horizontal* directions, in agreement with the notation used in most numerical and theoretical papers, even if the 'longitudinal' direction actually is the streamwise one in the experiment. For convenience (improving the collapse of experimental plots), each quantity can be plotted versus a 'fictitious' longitudinal Rossby number $R^*_o = (u'/L)|_{\Omega=0}/(2\Omega)$ which is the ratio u'/L of the non-rotating case divided by twice the actual rotation rate. The length and velocity scales u' and L, from the non-rotating case, that are used in this definition are time-dependent quantities. Thanks to this procedure, the transition point is rescaled to a single value for all data, independently of the different initial conditions and different rotation rates.

(ii) A longitudinal and a transverse 'two-dimensional energy component'

$$E^v_v = E^3_{33} = \langle u_3^2\rangle L^3_{33}\,, \qquad E^v_h = 2E^3_{11} = 2\langle u_1^2\rangle L^3_{11} \tag{4.3}$$

(equal in isotropic turbulence, see also Cambon 1990 for a discussion of the generalized 'two-dimensional energy components' $E^l_{ij} = \langle u_i u_j\rangle L^l_{ij}$).

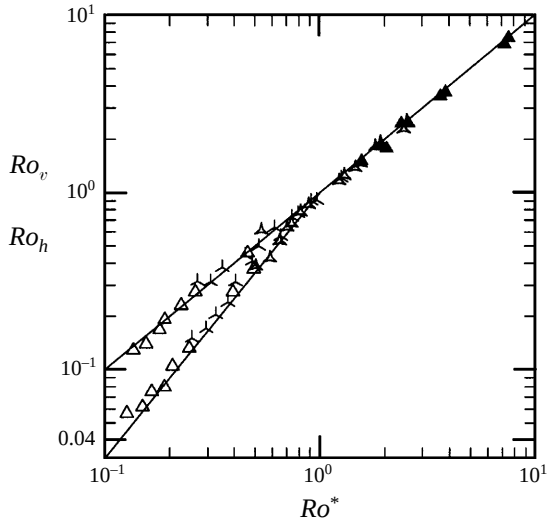

FIGURE 4. Evolution of Rossby numbers Ro_v (slope equal to 1) and Ro_h (slope equal to 1.5 after the transition). (Experiment by Jacquin.)

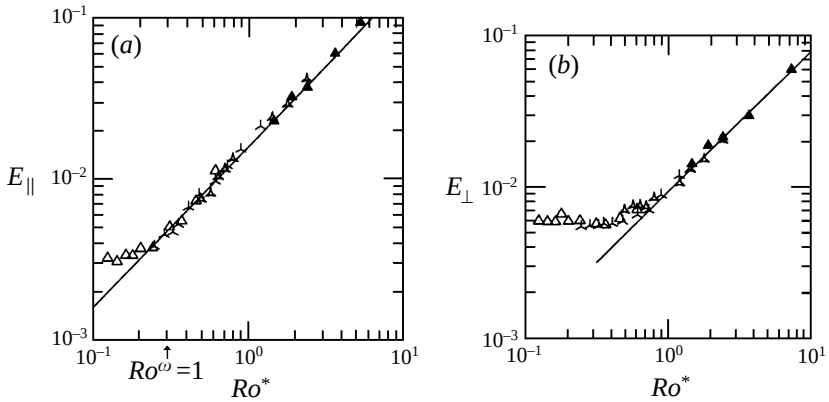

FIGURE 5. Evolution of (*a*) vertical non-dimensional energy $E_\parallel = E_v^v$ and (*b*) horizontal non-dimensional (i.e. divided by $\Omega U M^2$) energy $E_\perp = E_h^v$. (Experiment by Jacquin.)

The experimental results, predicted by the EDQNM2 results, showed that, at sufficiently high Reynolds number, Ro_v is unaffected by rotation and decays as t^{-1}, like the fictitious Rossby number (or u'/L without rotation), whereas Ro_h exhibits a sudden change of slope for a fictitious or (actually the longitudinal) macro-Rossby number close to 1, and decays as $t^{-1.5}$ for smaller values of the fictitious Rossby number (see figure 4 from Jacquin *et al.* 1989, 1990). The collapse is not so good for all of the data, but is, however, impressive for the two 'two-dimensional energy components' divided by the rotation rate and plotted in terms of the fictitious Rossby number. As shown in figure 5, E_h^v suddenly separates from E_v^v at the fictitious (or actual longitudinal) Rossby number close to 1 and is quasi-constant at smaller values. (Note that the scaling of the two-dimensional energy components in figure 5 in terms of $\Omega U M^2$, with U the streamwise mean velocity and M the mesh size, was suggested by the good collapse of E_h^v/Ω and E_h^h/Ω.) For smaller initial Reynolds numbers, such

as those reached in the Wigeland & Nagib (1978) experiment, this first transition, where anisotropy is triggered, can be delayed by viscous effects and occurred at macro-Rossby numbers smaller than 1. In Jacquin *et al.* (1990), the first transition is shown to occur at a macro-Rossby number smaller than unity if the Ekman number is higher than one at which the Reynolds number history curve crosses over the limit $Ro_v = 1$.

The evidence of a second transition which corresponds to the lower limit of the intermediate range of Rossby numbers (the range where nonlinear non-isotropic effects of rotation are statistically significant) comes also from experimental data (see again figure 5 and Jacquin *et al.* 1989, where a change in E_h^v is also exhibited near $Ro^\omega \sim 1$) but especially from EDQNM and DNS where high rotation rates are more easily reached. It is suggested that when a micro-Rossby number Ro^λ is smaller than 1, all the nonlinear effects become statistically insignificant, similar to the effects on the skewness in (3.5), so that the anisotropy can only evolve according to the so-called RDT solution and cannot be created. Even if resonant triads are selected at very low Rossby number, and tend to reduce the dimensionality, the measure of their manifold is statistically too weak to significantly influence the whole spectral transfer, which is more affected by the scrambling effect of non-resonant triads.

Hence, there exists a large body of evidence to support the simple scheme of an intermediate range of Rossby numbers limited by a macro-Rossby number (based on longitudinal quantities) close to 1 for the upper bound, and a micro-Rossby close to 1 for the lower bound. This range involves the Reynolds number through the ratio L/λ, and the upper limit can also be diminished at low Reynolds number, depending on the Ekman number.

In addition to the anisotropy indicators that involve the integral lengthscales, and especially the two-dimensional energy components, one can look at three-dimensional energy components: the anisotropy reflected by the Reynolds stress tensor and created at intermediate Rossby numbers was found weak but significant, especially in EDQNM2 results or in LES results at high Reynolds number.

4.2. *Exact relationship (without any closure)*

In agreement with equation (2.15), the real part of the second-order spectral tensor can be split into three parts:

$$\mathrm{Re}[\hat{U}_{ij}] = \frac{E}{4\pi k^2} P_{ij} + \left(e - \frac{E}{4\pi k^2} \right) P_{ij} + \mathrm{Re}[Z N_i N_j]. \tag{4.4}$$

Only the first term on the right-hand side characterizes a pure three-dimensional isotropic state, so that the two following terms are both anisotropic parts: the first involves the departure of e from a spherical distribution and thus characterizes a *directional anisotropy*, the second is trace free ($N_i N_i = 0$) and characterizes a polarization anisotropy (or tensorial anisotropy at a given wavevector). Any second-order correlation tensor in physical space can be found as the sum of three of these contributions. Accordingly a contribution from directional (superscript e) and polarization anisotropy (superscript z) is readily derived.

It is now interesting to distinguish the correlations in physical space which involve a three-dimensional integral from the ones which involve a two-dimensional integral.

Using (4.4), the Reynolds stress tensor is given by

$$\langle u_i u_j \rangle = q^2 \frac{\delta_{ij}}{3} + \int \left(e - \frac{E}{4\pi k^2} \right) P_{ij} \mathrm{d}^3 \boldsymbol{k} + \int \mathrm{Re}[Z N_i N_j] \mathrm{d}^3 \boldsymbol{k} \tag{4.5}$$

so that its deviatoric part $b_{ij} = \langle u_i u_j \rangle / q^2 - \delta_{ij}/3$ can be split as $b_{ij} = b^e_{ij} + b^z_{ij}$, where

$$q^2 b^e_{ij} = \int \left(e - \frac{E}{4\pi k^2} \right) P_{ij} \, \mathrm{d}^3 \boldsymbol{k} \tag{4.6}$$

also characterizes the anisotropy of the *dimensionality structure tensor* (Kida & Hunt 1989; Reynolds & Kassinos 1994):

$$D_{ij} = 2 \int \frac{k_i k_j}{k^2} e \, \mathrm{d}^3 \boldsymbol{k} = q^2 \left(\frac{\delta_{ij}}{3} - 2 b^e_{ij} \right). \tag{4.7}$$

The vorticity correlations can be derived from equations (2.15) and (4.5) by only changing e into $k^2 e$ and Z into $-k^2 Z$:

$$\langle \omega_i \omega_j \rangle = \int k^2 e P_{ij} - k^2 \mathrm{Re} \left[Z N_i N_j \right] \, \mathrm{d}^3 \boldsymbol{k}.$$

The two-dimensional energy components (Cambon 1990) $E^l_{ij} = \langle u_i u_j \rangle L^l_{ij}$ are given by a two-dimensional integral of eq. (2.15) for the spectral tensor in the wave-plane $k_l = 0$; the most interesting ones correspond to the plane $k_3 = 0$ where the 'rapid' effect of rotation is not present, or

$$E^v_v = E^3_{33} = \langle u_3^2 \rangle L^3_{33} = \pi \int (e + \mathrm{Re}[Z])|_{k_3=0} \, \mathrm{d}^2 \boldsymbol{k}, \tag{4.8}$$

$$E^v_h = E^3_{11} + E^3_{22} = \langle u_1^2 \rangle L^3_{11} + \langle u_2^2 \rangle L^3_{22} = \pi \int (e - \mathrm{Re}[Z])|_{k_3=0} \, \mathrm{d}^2 \boldsymbol{k}. \tag{4.9}$$

Other relationships for integral lengthscales with transverse separation and simplified equations for axisymmetric turbulence are available in Cambon & Jacquin (1989). It is worth noticing that neither the helicity spectrum nor the imaginary part of Z are involved in the above definitions of single-point correlations. In fact, helicity cannot be created in homogeneous turbulence with a centre of symmetry, and is relevant only in inhomogeneous flows, especially with strong spatial intermittency. On the other hand, the imaginary part of Z is present in the 'rapid' part (linear contribution) of the spectrum of the pressure–strain-rate tensor, in the presence of any rotational mean flow, and thus plays a role in the dynamics – especially the rapid effects – of some of the single-point correlations quoted above. In any case, Z must be interpreted as a complex term; in addition to its interpretation in terms of a correlation coefficient between the two helical mode intensities in (2.17), the modulus $|Z|$ is an invariant of the spectral tensor of double velocity – or vorticity – correlations, and its argument gives the orientation of the principal axis of the symmetrized spectral tensor at fixed $\boldsymbol{k}$, with respect to a given direction. Only in the waveplane $k_3 = 0$, is Z real, and $e+Z$ and $e-Z$ characterize spectral contributions from vertical and horizontal velocity components respectively, in agreement with (4.8) and (4.9).

Now, it is possible to predict the impact of the dynamics of e and Z (linear, then nonlinear) on the various correlations in physical space, using the exact relationships (4.5) to (4.9). The key equations for the prediction of the dynamics are the system (2.16) for e, Z, h. In the absence of nonlinear interactions, a regime expected for the micro-Rossby number smaller than 1, it is found that

$$\left.\begin{aligned} e(\boldsymbol{k},t) &= e(\boldsymbol{k},0) \exp(-2\nu k^2 t), \\ h(\boldsymbol{k},t) &= h(\boldsymbol{k},0) \exp(-2\nu k^2 t), \\ Z(\boldsymbol{k},t) &= Z(\boldsymbol{k},0) \exp(-2\nu k^2 t + 4\mathrm{i}\Omega t k_3/k). \end{aligned}\right\} \tag{4.10}$$

These linear solutions can be used for calculating the history of any second-order statistical quantity in accordance with the so-called RDT (Cambon & Jacquin 1989; Mansour *et al.* 1991*c*). Only Z, however, is actually affected by a 'rapid' timescale Ωt, and only for $k_3 \neq 0$. In addition, there is no distortion by the mean, so that the term RDT (rapid distortion theory) is not very relevant and will be replaced by linear approach in the following. Accordingly, if the Rossby number is small enough to separate a rapid and a slow timescale, the initial values in the above equations can be replaced by functions of the slow timescale, whose history is determined by the spectral transfer terms T^e, T^h, T^z in the system of equations (2.16).

The quantities which involve an integration along k_3 (or $\cos\theta_k$), such as the Reynolds stress tensor, the vorticity correlations tensor, or two-dimensional energy components in a plane other than $k_3 = 0$, must rapidly evolve until the contribution of the polarization anisotropy term Z is damped, whereas the part that involve e – thus the directional anisotropy $e(\boldsymbol{k}) - E(k)/(4\pi k^2)$ – will be conserved; the damping effect is due to the angular averaging of the phase term $\exp(4\mathrm{i}\Omega t k_3/k)$ in the linear solution (4.10). This behaviour is valid if the initial data are not too close to pure two-dimensional turbulence (as discussed below) and yield the rapid change of anisotropy reflected by the Reynolds stress tensor under rotation, as shown by several authors (Itsweire *et al.* 1979; Cambon & Jacquin 1989; Mansour *et al.* 1991*c*). Accordingly, any change in these quantities which involve the directional dependence of e is along the slow timescale; for instance the equality $b_{ij} = b^e_{ij}$ corresponds to a rapid damping of b^z_{ij}, whereas only the change in b^e_{ij} is along the slow timescale and reflects the transition towards the slow manifold (the two-dimensional state).

The quantities which involve integration over the wave-plane $k_3 = 0$ cannot exhibit any 'rapid' effect of rotation, so that the contributions from both e and Z deal with the slow timescale. The last step in the interpretation of anisotropic trends is to distinguish three cases:

(i) the pure three-dimensional three-component isotropic state (isotropy or 3D-3C)

$$e = \frac{E(k)}{4\pi k^2}\,, \qquad Z = h = 0 \tag{4.11}$$

(yielding $b_{ij} = b^e_{ij} = b^z_{ij} = 0$),

(ii) the pure two-dimensional two-component state (2D-2C)

$$e = \frac{E(k)}{2\pi k}\delta(k_3)\,, \qquad Z = -\frac{E(k)}{2\pi k}\delta(k_3)\,, \qquad h = 0 \tag{4.12}$$

(yielding $b_{33} = -1/3$, $b^e_{33} = 1/6$, $b^z_{33} = -1/2$).

(iii) the pure two-dimensional three-component state (2D-3C)

$$e = \frac{E(k)}{2\pi k}\delta(k_3)\,, \qquad Z = 0, h = 0 \tag{4.13}$$

(yielding $b_{33} = 1/6$, $b^e_{33} = 1/6$, $b^z_{33} = 0$).

In each case, as in intermediate anisotropic cases created by rotation, the components $b^{e,z}_{33}$ characterize the complete tensor in agreement with axisymmetry around $\Omega_i = \Omega\delta_{i3}$, or $b^{e,z}_{ij} = -3(\delta_{ij}/3 - \delta_{i3}\delta_{j3})b^{e,z}_{33}/2$.

4.3. *Nonlinear effects using EDQNM2 and LES results*

Starting with a pure 3D-3C isotropic state, it is clear that only the nonlinear effects reflected by (T^e, T^z) are capable of breaking the isotropy in the presence of rotation at intermediate Rossby numbers in order to create an axisymmetric state. The specific

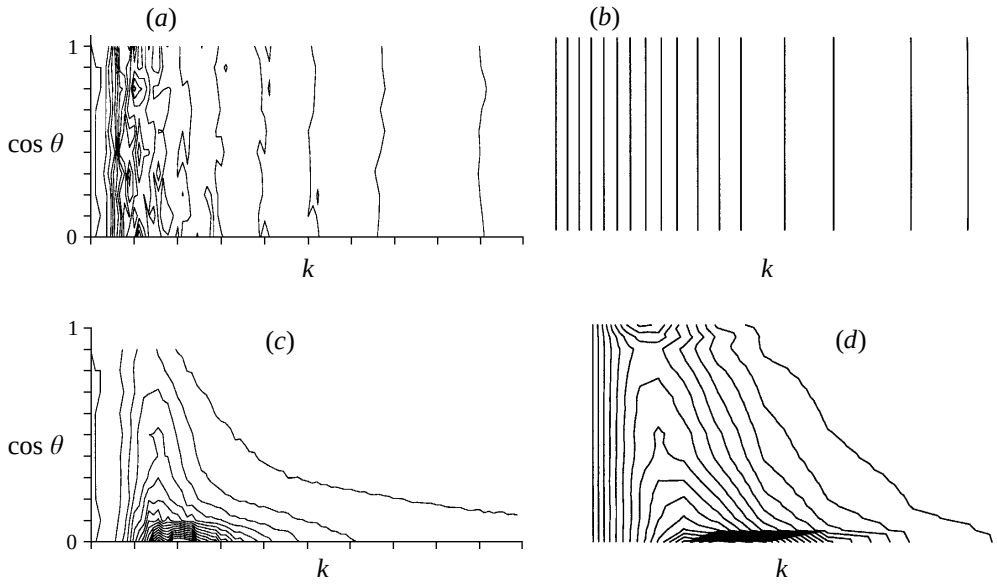

FIGURE 6. Isolines of kinetic energy for LES computations (*a*) at $\Omega = 0$ at time $t/\tau = 427$, (*b*) EDQNM2 with $\Omega = 0$; (*c*) LES with $\Omega = 1$ at $t/\tau = 575$; and (*d*) EDQNM2 calculation with $\Omega = 1$ at time $t/\tau = 148$.

development of the nonlinear terms T^e and T^z, and their impact on single-point quantities, will be shown using the CMS databases and the EDQNM2 model run at the same conditions: for two chosen values of the rotation rate ($\Omega = 0.5$ and $\Omega = 1$ dimensionalized with initial parameters box length $L = 2\pi$ and total (twice kinetic) energy $q^2 = 1$) and large initial Rossby numbers. The LES computations by CMS were run in a rectangular periodic box (of size $128 \times 128 \times 512$) to allow the vertical lengthscales to increase without affecting the periodic boundary condition assumption. The initial isotropic conditions were set at sufficiently large initial Rossby numbers to allow the triple correlations to develop before the linear role of rotation becomes important. In order to reach high Reynolds numbers, a spectral subgrid-scale model is used and molecular viscosity is omitted. The same SGS model is used in EDQNM2 equations, so that it is possible to compare the nonlinear interactions simulated from resolved scales in LES and their EDQNM modelling (through T^e and T^z in 2.16) with optimal accuracy.

The depiction of the energy density spectrum as a function of the modulus of the wavenumber is meaningful only when the energy distribution is isotropic. For the rotating case we expect the distribution of the energy density to be axisymmetric with respect to the k_3-axis and a function of $k_3/k = \cos\theta_k$. A natural coordinate system in this case is $k = (k_1^2 + k_2^2 + k_3^2)^{1/2}$ and k_3/k. An isotropic spectral distribution of the kinetic energy, will result in isolines parallel to the k-axis, with no dependence on θ_k, as shown in figure 6(*a*) for LES and figure 6(*b*) for EDQNM. In the latter case, the isolines are straight, since the isotropy is exactly described by this model. As the flow evolves, the angular-dependent nonlinear transfer accumulates energy towards the two-dimensional manifold (see §2.4), characterized by a wavevector orthogonal to the rotation axis, or equivalently $\theta_k = \pi/2$ (see figures 6*c* and 6*d*). There again, the strong similarity between EDQNM2 and LES plots appears even for this kind of representation which explicitly shows the detailed directional anisotropy. The

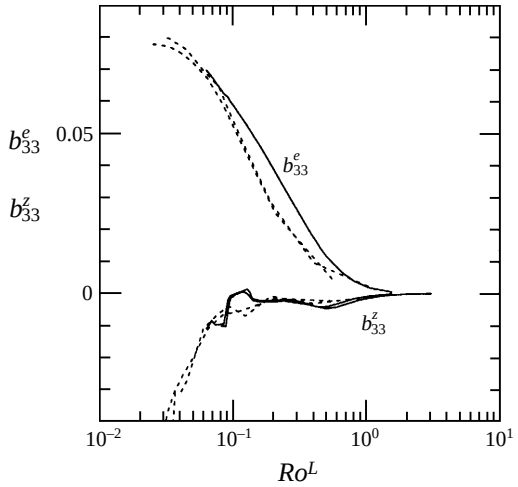

FIGURE 7. Variation of the anisotropy b^e_{33} and b^z_{33} with the Rossby number Ro^L, for $\Omega = 1$ and $\Omega = 0.5$, as given by: ——— , EDQNM2; - - - - , LES, computations.

highly concentrated energy region close to the equatorial plane (lower bound of the plot) would be roughly of the shape of a torus if one plotted its surface in the full three-dimensional spectral space. We can also notice that the discretization in LES for wavevectors close to $\cos\theta_k = 1$ is limited.

This concentration of spectral energy towards the wave-plane $k_3 = 0$ – the slow manifold – by T^e is a pure reduction of dimensionality (relative decrease of $\partial/\partial x_3$ in physical space) and affects only the directional dependence of e. Considered alone, this effect on dimensionality would create a ratio $\langle u_h^2\rangle/\langle u_v^2\rangle$ smaller than 1 (or equivalently $b_{33} > 0$), and would magnify the integral lengthscales with longitudinal separation, so that $E^3_{\alpha\alpha} > E^1_{\alpha\alpha}$ (no summation on α) for any velocity components; as an extremal state, the pure 2D-3C state (4.13) would give $\langle u_h^2\rangle/\langle u_v^2\rangle = 1/2$ (or $b_{33} = 1/6$) and $E^3_{ii} = \infty$. Therefore, regarding one-point quantities, the directional dependence is clearly seen on the e part of b_{33} (figure 7). The development of b^e_{33} as a function of the Rossby number shows a sudden increase in time when the critical value of Ro is reached, whereas the Z part b^z_{33} does not show a significant departure from its initial zero value. Note that at the smallest Rossby number, a sudden rise of negative b^z_{33} occurs; this effect, which is extensively discussed in CMS, is associated with a second transition ($Ro^\omega \sim 1$). This second transition is outside the scope of this paper.

Another anisotropic effect involves the 'polarization anisotropy transfer' T^z which, in addition to the angular dependence of energy, displays a polarization of the spectral energy at fixed $\boldsymbol{k}$ in terms of different contributions from vertical $\langle\hat{u}_3^*\hat{u}_3\rangle$ and horizontal $\langle\hat{u}_1^*\hat{u}_1\rangle + \langle\hat{u}_2^*\hat{u}_2\rangle$ velocity components. This effect cannot be predicted by Waleffe's analysis of §2, and is only obtained with EDQNM2 and high-Reynolds-number LES (Squires *et al.* 1994; CMS). This effect is detected in physical space by the 'de-coupling' between L^3_{33} and L^3_{11} (see figure 8 from CMS data), or more relevantly between E^v_h and E^v_v (4.8) and (4.9), as in the experiment by Jacquin *et al.* (1990). Equations (2.16), (4.8) and (4.9) clearly show that this effect on componentality is due to a rise of Z (only driven by T^z) in the wave-plane $k_3 = 0$, so that a possible 2D-3C state would evolve towards a 2D-2C state, where $E^v_h = \infty, E^v_v = 0$. It must be pointed out, however, that this tendency, 2D-3C $\rightarrow$ 2D-2C, only concerns the two-dimensional energy components, and not the Reynolds stress tensor in which

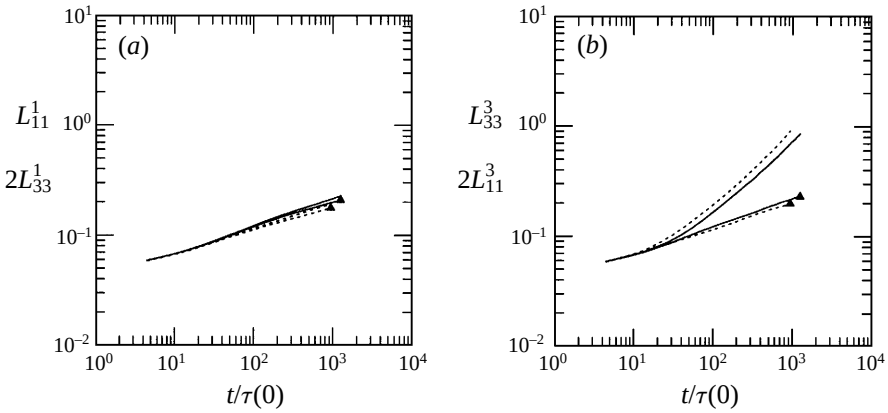

FIGURE 8. (*a*) Horizontal integral length scales; symbol indicate $2L_{33}^1$ curves, others for L_{11}^1. (*b*) Vertical integral length scales; symbol indicate L_{33}^3 curves, others for $2L_{11}^3 = L_{11}^3 + L_{22}^3$. – – – – , $\Omega = 1$; ——— , $\Omega = 0.5$.

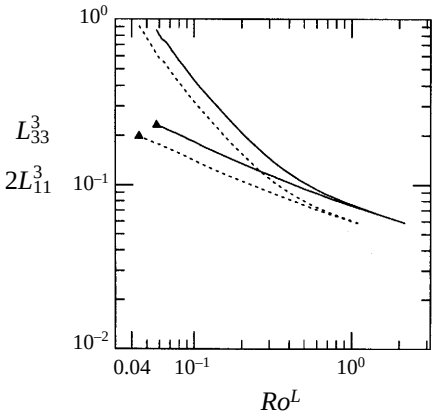

FIGURE 9. Vertical integral length scales as a function of the macro-Rossby number. Symbol indicates L_{33}^3 curves, others for $2L_{11}^3$. – – – – , $\Omega = 1$; ——— , $\Omega = 0.5$.

the dominance of the vertical component prevails. This transition of state may be well indicated by the range of the Rossby number in such a decreasing turbulence: a value around unity is the starting point for the anisotropic behaviour of nonlinear dynamics of the flow, as indicated by the experimental data in figures 5(*b*) and 4, or in figure 9 for EDQNM2 results. It is interesting to see that in his experiments, in order to collapse all the experimental points onto one curve, Jacquin was led to define the energy components $E_\perp$ and $E_\parallel$ as non-dimensionalized by the mean velocity of the flow and the grid mesh size, but also by the rotation rate Ω (figure 5). Doing so for $\langle u_3^2 \rangle L_{33}^3$ and $\langle u_1^2 \rangle L_{11}^3 + \langle u_2^2 \rangle L_{22}^3$, given by LES and EDQNM2, collects all the results under one curve for each component, and one easily sees that the transition (separation point of the two energy-component curves) appears at the same time for both (see figure 10). However, the LES predicts a more important tendency than the EDQNM2 model (figure 10*b*), for which the rate of departure of the two components is less. But the increase of $\langle u_1^2 \rangle L_{11}^3 + \langle u_2^2 \rangle L_{22}^3$ shown by the LES evolution does not appear in the experimental data of figure 5.

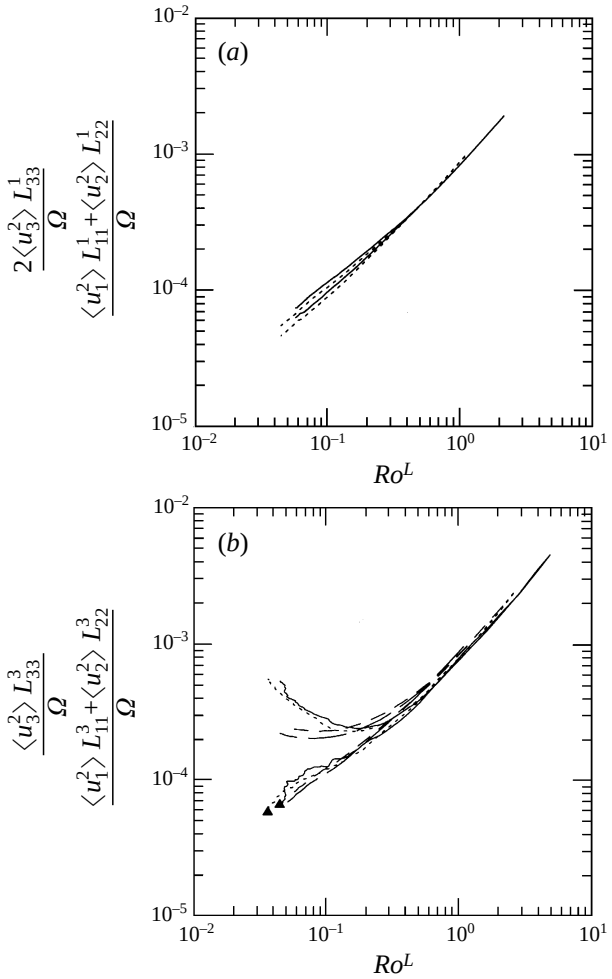

FIGURE 10. (*a*) Horizontal components of Reynolds stress tensor times the corresponding integral length scale: energy components, divided by Ω. Symbol indicates $2\langle u_3^2\rangle L_{33}^1$ curves, others for $\langle u_1^2\rangle L_{11}^1 + \langle u_2^2\rangle L_{22}^1$; EDQNM2: – – – – , $\Omega = 1$; ——— , $\Omega = 0.5$. (*b*) Vertical components of Reynolds stress tensor times the corresponding integral length scale: symbol indicates $\langle u_3^2\rangle L_{33}^3$ curves, others for $\langle u_1^2\rangle L_{11}^3 + \langle u_2^2\rangle L_{22}^3$. LES: – – – – , $\Omega = 1$; ——— , $\Omega = 0.5$. EDQNM2: ——— — , $\Omega = 1$; – – – – , $\Omega = 0.5$.

5. Conclusion

Organized around the main theme of the importance of nonlinear effects on the dynamics of turbulence subjected to solid-body rotation, the contents of this paper are two-fold: first we investigated the extent of applicability of weakly nonlinear theories for wave turbulence, as well as their relationships to high-Reynolds-number modelling of turbulence; second, we have shown that the effects of rotation on one-point and two-point statistics are through nonlinear interactions. It is shown that a spectral description (or two-point modelling) is needed to capture the effects of rotation. Separating the linear effects of rotation on turbulence from the nonlinear ones leads to a detailed investigation of nonlinear energy transfers. We have shown that in order to account for the effects of rotation on a one-point closure, the effects of rotation on the triple correlations has to be taken into account through the skewness.

The skewness is shown to be strongly damped by the rotation in both EDQNM2 and DNS results. The simpler EDQNM model corrected for rotation is shown to be able to capture the effects of rotation on the skewness. The definition of a new micro-Rossby number Ro^{ω} proves useful regarding the collapse of all the skewnesses on the same curve, with a given analytical expression $S^{e}(Ro^{\omega})$. The critical value of 1 for Ro^{ω} is the limit for recovering a regime of pure viscous decay.

We then reviewed the anisotropic effects of nonlinearity in rotating flows, namely a directional anisotropy that tends to accumulate energy in the spectral direction orthogonal to the external rotation vector (the two-dimensional domain or slow manifold), a process that can be partly explained by an instability analysis (Waleffe), and for which evidence has been found in EDQNM2 distribution of the energy spectrum e (Cambon & Jacquin 1989), in experimental data (Jacquin *et al.* 1989, 1990), in LES computations (CMS) and in DNS computations (Mansour *et al.* 1991*a*, *b*) but less clearly.

This spectral accumulation of energy towards the slow manifold, when the macro-Rossby number reaches 1, is the beginning of a transition from a pure three-dimensional state to a two-dimensional one: the directional anisotropy is consistent with a lessening of the dimensionality in rotating flows. We have shown that the spectral decomposition into energy e and polarization anisotropy Z spectra retains the full anisotropic information, which, by selected integrations in spectral space, gives the directional anisotropy indicator in physical space, namely the deviatoric part b_{ij} of the Reynolds stress tensor. The latter, when decomposed into the two contributions b^{e}_{ij} and b^{z}_{ij} also shows the transition, through a sudden increase in b^{e}_{ij}.

The two transitions cannot be explained by separating 'rapid' linear terms, with a scaling Ωt, from 'slow' nonlinear terms, suggested by the analysis of wave turbulence in §2. This separation is not relevant in the intermediate range of Rossby numbers. Indeed, the terms that reflect nonlinear interactions can also involve the 'rapid' non-dimensional time Ωt (see for example the scaling laws in Squires *et al.* 1994, confirmed by LES results, and consistent with an energy transfer proportional to the short timescale $1/\Omega$). As mentioned before, a possible interpretation of the scaling of the nonlinear energy transfer in terms of $1/\Omega$ is the dominant role of non-resonant triads, through a phase scrambling of interacting inertial waves, with respect to resonant triads. In other words, resonant triads are useful for a qualitative analysis of weak nonlinear trends towards two-dimensionalisation, but are of no relevance from a statistical point of view, in strong turbulence, since they then do not clearly emerge. The inhibition of the energy cascade, which can be predicted by simple isotropic models in §3 (from EDQNM to k–ε), is consistent with such a weighting in $1/\Omega$ of the averaged energy transfer, and this behaviour can be found without any significant trend towards bidimensionalization occurring. For the flow we considered, the only quantity which could be directly related to the slow time behaviour of the resonant triads is $E^{v}_{h} = \langle u_1^2 \rangle L^3_{11} + \langle u_2^2 \rangle L^3_{22}$, which involves the horizontal velocity components in the horizontal waveplane (the slow manifold). The strong increase of this quantity in LES (CMS), whose behaviour seems to be decoupled from all other statistical quantities, could reveal the emergence of an inverse energy cascade, characteristic of a pure two-dimensional dynamics ($k_3 = p_3 = q_3 = 0$). The problem is not easy, however, since even the nonlinear dynamics of quantities that involve the slow manifold ($k_3 = 0$) depend on other wavevector directions through triadic integrals (with $p_3 = -q_3 \neq 0$). The analysis of Waleffe suggests that the pure two-dimensional manifold is decoupled, at the lowest order of a formal Rossby number, but the numerical approaches at finite Rossby number are not conclusive, and different

numerical and theoretical problems can interfere: accounting for the zero- or low-dimension manifolds in discretized wavespace is not obvious, and a Rossby number has no local meaning in pure two-dimensional equations ($k_3 = p_3 = q_3 = 0$), since rotation terms vanish in (2.6) and (2.10).

By examining the evolution of the anisotropic indicators in physical space, using both CMS LES databases and EDQNM2, we have confirmed (CMS) the existence of an intermediate range of Rossby numbers. The upper bound is characterized by a macro-Rossby number $Ro^L = u'/(2\Omega L_{33}^3)$ whose value close to 1 is linked to a first transition towards two-dimensionalization. Starting from an initially 3D isotropic turbulence decaying in the presence of rotation (with obviously $Ro^L > 1$ initially and given a large Reynolds number) the anisotropy is suddenly triggered at $Ro^L = 1$. Note that most of the DNS rotating cases by Mansour *et al.* (1991*a*, *b*), even for 256^3, corresponded to histories that started inside the intermediate range of Rossby numbers. For the few cases with initially (end of the precomputation) $Ro^L > 1$, the transition was delayed and the resulting anisotropy was small. On the other hand, a clear first transition is exhibited using the LES databases of CMS. The first explicit mention of the second transition was given by Jacquin *et al.* (1989), on the grounds of an analogy with the role of the Osmidov lengthscale in stably stratified turbulence. The exact value of the corresponding lower bound of the intermediate range of Rossby number characterizes a complete damping of nonlinear interactions for $Ro^\lambda \ll 1$ – in contradiction to a well-known interpretation of the Taylor–Proudman theorem. A complete discussion of its relation to the Osmidov scale for both transitions is given by CMS.

Finally, the whole study confirms the relevance of the spectral formalism (e, Z, h) for characterization of complex and detailed anisotropic features. The development of the anisotropy is a prelude to a trend towards two-dimensionalization. We have pointed out that the polarization anisotropy Z is a component of the anisotropy that is poorly reflected in the representation of anisotropy in 'classic' one-point correlations. Quantities such as $\langle u_3^2\rangle L_{33}^3$ or $\langle u_1^2\rangle L_{11}^3 + \langle u_2^2\rangle L_{22}^3$ are influenced by the Z-term.

C.C. and F.S.G. would like to acknowledge partial support of the Center for Turbulence Research during the course of this study. Many discussions with Professors K. Squires and J. Chasnov are also gratefully acknowledged.

Appendix. The EDQNM2 model

The EDQNM2 model was introduced to take into account additional linear operators in the governing equations for velocity or temperature fields. The general – semi-symbolic – closure relation for the spectral tensor of triple correlations at two points reads

$$\langle \hat{u}_{\cdot}(\boldsymbol{k},t)\hat{u}_{\cdot}(\boldsymbol{p},t)\hat{u}_{\cdot}(\boldsymbol{q},t)\rangle = \int_0^t \int_{\boldsymbol{k}+\boldsymbol{p}+\boldsymbol{q}=0} G_{\cdot\cdot}^{ED}(\boldsymbol{k},t,t')M_{\cdot\cdot\cdot}(\boldsymbol{k},\boldsymbol{p},\boldsymbol{q}) \times [G_{\cdot\cdot}^{ED}(\boldsymbol{p},t,t')\hat{U}_{\cdot\cdot}(\boldsymbol{p},t)][G_{\cdot\cdot}^{ED}(\boldsymbol{q},t,t')\hat{U}_{\cdot\cdot}(\boldsymbol{q},t)]\ \mathrm{d}^3\boldsymbol{p}\ \mathrm{d}t' + \ldots \quad (A\,1)$$

where $\boldsymbol{G}^{ED}(\boldsymbol{k},t,t')$ is similar to the Kraichnan response tensor, and chosen as the product of the tensor $\boldsymbol{G}$ that generates the exact linear solution (the zero-order response tensor) and an *ad hoc* eddy-damping term. $\hat{\boldsymbol{U}}$ is the second-order spectral tensor at time t, and $\boldsymbol{M}$ is the 'influence matrix' that characterizes the basic nonlinearity in spectral space. For the sake of brevity, the subscripts are omitted in the above symbolic equation, and the dots at the end stand for two similar terms obtained by

circular permutation of the vectors of the triad. Finally a transient term linked with a possible initial value (time $t = 0$) of triple correlations is omitted too.

The above equation can be written in any orthonormal frame of reference (for $\boldsymbol{k}, \boldsymbol{p}, \boldsymbol{q}$) and especially in the eigenframe in which $\boldsymbol{G}$ is diagonal. Accordingly, the time integral of the product of the three response tensors yields the term $\theta_{kpq}^{\epsilon\epsilon'\epsilon''}$ in equation (2.21) as the generalized triadic characteristic time, that is the weighting factor of any quasi-normal expansions in generalized transfer terms. In addition, the contributions from the spectral tensor related to $\boldsymbol{k}, \boldsymbol{p}, \boldsymbol{q}$ amount to the sets (e, Z), (e', Z'), (e'', Z'') in the eigenframe, respectively. The last main change of frame, which allows a separation between moduli and orientation, and is also a key in the Waleffe analysis reported in §2, consists of rotating the three eigenframes related to $\boldsymbol{k}, \boldsymbol{p}, \boldsymbol{q}$ by angles $\lambda, \lambda', \lambda''$ in order to refer them to a polar axis linked to the plane of the triad, rather than a polar axis with a fixed (vertical) direction. The three angles give the angles between the plane of the triad and the three vectors $\boldsymbol{k}, \boldsymbol{p}, \boldsymbol{q}$, respectively. Thus, the spectral tensor contributions become

$$\left.\begin{aligned} e = e(\boldsymbol{k}, t), \quad X &= Z(\epsilon\boldsymbol{k}, t)\mathrm{e}^{2\mathrm{i}\epsilon\lambda}, \\ e' = e(\boldsymbol{p}, t), \quad X' &= Z(\epsilon'\boldsymbol{p}, t)\mathrm{e}^{2\mathrm{i}\epsilon'\lambda'}, \\ e'' = e(\boldsymbol{q}, t), \quad X'' &= Z(\epsilon''\boldsymbol{q}, t)\mathrm{e}^{2\mathrm{i}\epsilon''\lambda''}, \end{aligned}\right\} \tag{A 2}$$

and the influence matrix (equation (2.7)) becomes

$$M_{\epsilon\epsilon'\epsilon''} = m_{\epsilon\epsilon'\epsilon''}(k, p, q)\mathrm{e}^{\mathrm{i}(\epsilon\lambda+\epsilon'\lambda'+\epsilon''\lambda'')}$$

so that the orientation is only involved in the three angles $(\lambda, \lambda', \lambda'')$, in $\theta_{kpq}^{\epsilon\epsilon'\epsilon''}$ (for the rotating case) and in the basic terms (e, Z) (if anisotropy develops) but not in most of the geometrical coefficients, given below, that only depend on (k, p, q). Finally it is found that

$$\begin{aligned} T^e = \frac{1}{2^3}\sum_{\epsilon\epsilon'\epsilon''}\int \frac{2p}{k}\, C_{kpq}^2\theta_{kpq}^{\epsilon\epsilon'\epsilon''} \big[& A_1(\epsilon k, \epsilon' p, \epsilon'' q)e''(e - e') \\ & + A_2(\epsilon k, \epsilon' p, \epsilon'' q)eX'' + A_3(\epsilon k, \epsilon' p, \epsilon'' q)e''X \\ & - A_5(\epsilon k, \epsilon' p, \epsilon'' q)e'X'' + A_4(\epsilon k, \epsilon' p, \epsilon'' q)X''(X - X')\big]\ \mathrm{d}^3\boldsymbol{p}, \end{aligned} \tag{A 3}$$

$$\begin{aligned} T^z = \frac{1}{2^3}\sum_{\epsilon'\epsilon''}|_{\epsilon=1}\int \frac{2p}{k}\, C_{kpq}^2\mathrm{e}^{-2\mathrm{i}\lambda}\theta_{kpq}^{\epsilon\epsilon'\epsilon''} \big[& A_3(k, -\epsilon' p, -\epsilon'' q)e''(e' - e) \\ & + A_4(k, -\epsilon' p, -\epsilon'' q)eX'' + A_1(k, -\epsilon' p, -\epsilon'' q)e''X \\ & - A_5(k, -\epsilon' p, -\epsilon'' q)e''X' + A_2(k, -\epsilon' p, -\epsilon'' q)X''(X - X')\big]\ \mathrm{d}^3\boldsymbol{p} \end{aligned} \tag{A 4}$$

where e, X, e', X', e'', X'' are given in (A 2) and the geometric coefficients are

$$\left.\begin{aligned} C_{kpq} &= \frac{\sin(p, q)}{k} = \frac{\sin(q, k)}{p} = \frac{\sin(k, p)}{q}, \\ A_1(k, p, q) &= -(p - q)(k + p + q)(k - q)(k + p + q), \\ A_2(k, p, q) &= -(p - q)(k + p + q)(k + q)(k + p - q), \\ A_3(k, p, q) &= (p - q)(k + p + q)(k + q)(-k + p + q), \\ A_4(k, p, q) &= (p - q)(k + p + q)((k - q)(k - p + q), \\ A_5(k, p, q) &= -(p - q)(k + p + q)(p + q)(k + p - q). \end{aligned}\right\} \tag{A 5}$$

The coefficients linked to 'output terms' $a(\boldsymbol{p},t)b(\boldsymbol{q},t)$ may have a different form, given the symmetry between $\boldsymbol{p}$ and $\boldsymbol{q}$ in the integrals (A 3) and (A 4).

If the rotation is taken out, $\theta_{kpq}^{\epsilon\epsilon'\epsilon''}$ reduces to θ_{kpq} and the summation on the polarity signs $\epsilon,\epsilon',\epsilon'',=+1,-1$ yields the following simplified terms:

$$T^e = \int \theta_{kpq}\, 2kp \left[(e''+\mathrm{Re}X'')\left[(xy+z^3)(e'-e)-z(1-z^2)(\mathrm{Re}X'-\mathrm{Re}X)\right]\right.$$
$$\left. +\,\mathrm{Im}X''(1-z^2)(x\,\mathrm{Im}X-y\,\mathrm{Im}X')\right]\ \mathrm{d}^3\boldsymbol{p} \qquad (A\,6)$$

$$T^z = \int \theta_{kpq}\, 2kp\, e^{-2\mathrm{i}\lambda} \left[(e''+\mathrm{Re}X'')\left[(xy+z^3)(\mathrm{Re}X'-X)-z(1-z^2)(e'-e)\right.\right.$$
$$\left.\left. +\mathrm{i}\,(y^2-z^2)\,\mathrm{Im}X'\right]+\mathrm{i}\,\mathrm{Im}X''(1-z^2)(x(e+X)-\mathrm{i}\,y\,\mathrm{Im}X')\right]\ \mathrm{d}^3\boldsymbol{p} \qquad (A\,7)$$

where the geometric coefficients are instead expressed in terms of the cosines of the inner angles of the triangle (k,p,q), $x=\cos(p,q)$, $y=\cos(q,k)$, $z=\cos(k,p)$, using $C_{kpq}^2 kp = xy+z, C_{kpq}^2 q^2 = 1-z^2$, for instance. Finally, the triadic integrals in (A 3), (A 4), (A 6), and (A 7) can be solved using the following change of variables:

$$\int S(\boldsymbol{k},\boldsymbol{p},t)\ \mathrm{d}^3\boldsymbol{p} = \int_{\Delta_k}\left[\int_0^{2\pi} S'(\boldsymbol{k},p,q,\lambda)\ d\lambda\right]\frac{pq}{k}\ \mathrm{d}p\ \mathrm{d}q$$

where Δ_k is the domain of p and q so that k,p,q are the lengths of the sides of a triangle. Equations (A 6) and (A 7) characterize the EDQNM1 model, without the explicit effect of mean gradient or body forces, for any anisotropic configuration (Benoit 1992).

Classic EDQNM expressions for the isotropic (3D-3C) case (where $e=E(k,t)/(4\pi k^2)$, $T^e = T(k,t)/(4\pi k^2)$, $T^z = Z = 0$) and for the (2D-2C) case (Pouquet *et al.* 1975) are easily recovered from (A 6) and (A 7). Only the first term $e''(e'-e)$ on the left-hand side of (A 6), is present in the three-dimensional isotropic case, and the simplified model in §3.1 is derived from the corresponding expression for $T = 4\pi k^2 T^e$ by changing θ_{kpq} only, as in (2.17). This yields the integrand $S^{QN} = 16\pi^2 k^2 pq(xy+z^3)e''(e'-e)$ in (2.19).

The (2D-3C) model of Cambon & Godeferd (1993) is also derived from (A 6) and (A 7) in terms of $(e-Z)|_{k_3=0}$ (horizontal velocity contribution in the slow manifold) and $(e+Z)|_{k_3=0}$ (vertical velocity contribution in the slow manifold), accounting for rotation effects vanishing in the two-dimensional limit and that $\int \mathrm{d}^2\boldsymbol{p} = \int_{\Delta_k}[\sin(p,q)]^{-1}\mathrm{d}p\mathrm{d}q$ and $\mathrm{e}^{2\mathrm{i}\lambda} = \mathrm{e}^{2\mathrm{i}\lambda'} = \mathrm{e}^{2\mathrm{i}\lambda''} = -1$.

REFERENCES

André, J. C. & Lesieur, M. 1977 Influence of helicity on high Reynolds number isotropic turbulence. *J. Fluid Mech.* **81**, 187–207.

Aupoix, B. 1984 Eddy viscosity subgrid-scale models for homogeneous turbulence. In *Proc. Macroscopic Modelling of Turbulent Flows*. Lecture Notes in Physics, vol. 230, pp. 45–50. Springer.

Bardina, J., Ferziger, J. M. & Rogallo, R. S. 1985 Effect of rotation on isotropic turbulence: computation and modelling. *J. Fluid Mech.* **154**, 321–336.

Bartello, P., Métais, O. & Lesieur, M. 1994 Coherent structures in rotating three-dimensional turbulence. *J. Fluid Mech.* **273**, 1–29.

Batchelor, G. K. 1953 *The Theory of Homogeneous Turbulence*. Cambridge University Press.

Benney, D. J. & Saffman, P. G. 1966 Nonlinear interactions of random waves in a dispersive medium. *Proc. R. Soc. Lond.* A **289**, 301–320.

Benoit, J. P. 1992 Étude expérimentale et théorique d'une turbulence homogène soumise à des effets couplés de rotation et déformation plane. Thèse de doctorat, École Centrale de Lyon.

Cambon, C. 1982 Étude spectrale d'un champ turbulent incompressible soumis à des effets couplés de déformation et de rotation imposés extérieurment. *Thèse d'état*, Université Lyon I.

Cambon, C. 1990 Single and two point modelling of homogeneous turbulence. *Annual Research Briefs*. Center for Turbulence Research, Stanford University.

Cambon, C., Bertoglio, J. P. & Jeandel, D. 1981 Spectral closure of homogeneous turbulence. *AFOSR–Stanford Conf. on Complex Turbulent Flows.*

Cambon, C. & Godeferd, F. S. 1993 Inertial transfers in freely decaying, rotating, stably stratified and MHD turbulence. In *Progress in Astronautics and Aeronautics* (ed. H. Branover & Y. Unger). AIAA.

Cambon, C. & Jacquin, L. 1989 Spectral approach to non-isotropic turbulence subjected to rotation. *J. Fluid Mech.* **202**, 295–317.

Cambon, C., Jacquin, L. & Lubrano, J.-L. 1992*a* Toward a new Reynolds stress model for rotating turbulent flows. *Phys. Fluids* A **4**, 812–824.

Cambon, C., Mansour, N. N. & Squires, K. D. 1994 Anisotropic structure of homogeneous turbulence subjected to uniform rotation. *Center for Turbulent Research Proc. Summer Program* (referred to herein as CMS).

Cambon, C., Mao, Y. & Jeandel, D. 1992*b* On the application of time dependent scaling to the modelling of turbulence undergoing compression. *Eur. J. Mech.* B *Fluids* **11**, 683–703.

Chasnov, J. 1994 Similarity states of passive scalar transport in isotropic turbulence. *Phys. Fluids* **6**, 1036–1051.

Chollet, J. P. & Lesieur, M. 1981 Parameterization of small scales of three-dimensional isotropic turbulence utilizing spectral closures. *J. Atmos. Sci.* **38**, 2747–2757.

Craya, A. 1958 Contribution à l'analyse de la turbulence associée à des vitesses moyennes. *P.S.T. Ministère de l'Air* 345.

Dang, K. & Roy, Ph. 1985 Direct and large eddy simulations of homogeneous turbulence submitted to solid body rotation. *Proc. Turbulent Shear Flows 5, August 7–9, 1985 Cornell University Ithaca*, pp. 17-1–17-6.

Godeferd, F. S. & Cambon, C. 1994 Detailed investigation of energy transfers in homogeneous stratified turbulence. *Phys. Fluids* **6**, 2084–2100.

Greenspan, H. P. 1968 *The Theory of Rotating Fluids.* Cambridge University Press.

Hasselmann, K. 1962 On the non-linear energy transfer in a gravity-wave spectrum. Part 1. General theory. *J. Fluid Mech.* **12**, 481–500.

Herring, J. R. 1974 Approach of axisymmetric turbulence to isotropy. *Phys. Fluids* **17**, 859.

Hopfinger, E. J., Browand, F. K. & Gagne, Y. 1982 Turbulence and waves in a rotating tank. *J. Fluid Mech.* **125**, 505–534.

Itsweire, E., Chabert, L. & Gence, J. N. 1979 Action d'une rotation pure sur une turbulence homogène anisotrope. *C. R. Acad. Sci. Paris* **289B**, 197.

Jacquin, L. 1987 Etude théorique et expérimentale de la turbulence homogène en rotation. Thèse de Doctorat d'État, Université Claude Bernard–Lyon I.

Jacquin, L., Leuchter, O., Cambon, C. & Mathieu, J. 1990 Homogeneous turbulence in the presence of rotation. *J. Fluid Mech.* **220**, 1–52.

Jacquin, L., Leuchter, O. & Geoffroy, P. 1989 Experimental study of homogeneous turbulence in the presence of rotation. *Turbulent Shear Flows 6*. Springer.

Kida, S. & Hunt, J. C. R. 1989 Interaction between different scales of turbulence over short times. *J. Fluid Mech.* **201**, 411–445.

Kraichnan, R. H. 1976 Eddy viscosity in two and three dimensions. *J. Atmos. Sci.* **33**, 1521–1536.

Lorenz, E. N. 1980 Attractor sets and quasi-geostrophic equilibrium. *J. Atmos. Sci.* **37**, 1685–1699. Springer.

Mansour, N. N., Cambon, C. & Speziale C. G. 1991*a* Theoretical and computational study of rotating isotropic turbulence. *Studies in Turbulence* (ed. T. B. Gatski, S. Sarkar & C. G. Speziale). Springer.

Mansour, N. N., Cambon, C. & Speziale C. G. 1991*b* Single point modelling of initially isotropic turbulence under uniform rotation. *Annual Research Briefs*. Center for Turbulence Research, Stanford University.

Mansour, N. N., Shih, T.-H. & Reynolds, W. C. 1991*c* The effects of rotation on initially anisotropic homogeneous flows. *Phys. Fluids* A **3**, 2421–2425.

Mansour, N. N. & Wray, A. A. 1994 Decay of isotropic turbulence in low Reynolds number. *Phys. Fluids* **6**, 808–814.

Orszag, S. A. 1970 Analytical theories of turbulence. *J. Fluid Mech.* **41**, 363–386.

Pedlosky, J. 1986 *Geophysical Fluid Dynamics,* 2nd Edn, pp. 160–163. Springer.

Pouquet, A., Lesieur, M., André, J. C. & Basdevant, C. 1975 Evolution of high Reynolds number two-dimensional turbulence. *J. Fluid Mech.* **72**, 305–320.

Proudman, J. 1916 On the motion of solids in a liquid possessing vorticity. *Proc. R. Soc. Lond.* A **92**, 408.

Reynolds, W. C. & Kassinos, S. 1994 A one-point model for the evolution of the Reynolds stress and structure tensors in rapidly deformed homogeneous turbulence. *Osborne Reynolds Centenary Symposium.* UMIST Manchester, UK.

Rogallo, R. S. 1981 Numerical experiments in homogeneous turbulence. *NASA Tech. Mem.* 81315.

Speziale, C. G., Mansour, N. N., Rogallo, R. S. 1987 Decay of turbulence in a rapidly rotating frame. *Proc. 1987 Summer Program, CTR*, Rep. CTR–S87, pp. 205–212.

Squires, K. D., Chasnov, J. R., Mansour, N. N. & Cambon, C. 1993 Investigation of the asymptotic state of rotating turbulence using large-eddy simulation. *Annual Research Briefs*, pp. 157–170. Center for Turbulence Research, Stanford University.

Squires, K. D., Chasnov, J. R., Mansour, N. N. & Cambon, C. 1994 The asymptotic state of rotating homogeneous turbulence at high Reynolds numbers. *AGARD CP* 551, pp. 4-1–4-9.

Taylor, G. I. 1921 Experiments on the motion of solid bodies in rotating fluids. *Proc. R. Soc. Lond.* A **104**, 213.

Teissèdre, C. & Dang, K. 1987 Anisotropic behaviour of rotating homogeneous turbulence by numerical simulation. *AIAA Paper* 87-1250.

Veeravalli, S. V. 1991 An experimental study of the effects of rapid rotation on turbulence. *Annual Research Briefs.* NASA-Stanford Center for Turbulence Research.

Wigeland, R. A. & Nagib, H. M. 1978 Grid generated turbulence with and without rotation about the streamwise direction. *IIT Fluids and Head Transfer Rep.* R78-1.

Waleffe, F. 1991 Non-linear interactions in homogeneous turbulence with and without background rotation. *Annual Research Briefs.* Center for Turbulence Research, Stanford University.

Waleffe, F. 1993 Inertial transfer in the helical decomposition. *Phys. Fluids* A **5**, 677–685.

Zimont, V. L. & Sabelńikov, V. A. 1975 On turbulent diffusion of passive scalar in sheared homogeneous turbulent flows. *Izv. Akad. Neuk. SSSR, Mekh. Zhid. i Gaza* **6**, 22–29 (In Russian.)